https://doi.org/10.5194/se-2020-127
Preprint. Discussion started: 27 August 2020
© Author(s) 2020. CC BY 4.0 License.

Solid Earth Discussions

Thick- and thin-skinned basin inversion in the Danish Central Graben, North Sea – the role of deep evaporites and basement kinematics

Torsten Hundebøl Hansen[1], Ole Rønø Clausen[1], Katrine Juul Andresen[1]

[1]Department of Geoscience, Aarhus University, Aarhus C, 8000, Denmark

Correspondence to: Torsten Hundebøl Hansen (torsten.h.hansen@geo.au.dk)

Abstract. Using 3D reflection-seismic data constrained by wells, we address the kinematic connections between Permian Zechstein evaporites, basin-inversion structures in the sedimentary units above, and reactivated structures in the sub-salt basement in the Danish Central Graben. The Danish Central Graben is part of the failed North Sea rift system. Where present, mobile Zechstein evaporites have played a significant role in its structural development since the Triassic, while tectonic shortening caused mild inversion in the Late Cretaceous and Paleogene. Shortening was accommodated mainly by reverse reactivation of older normal faults (i.e. fault inversion) along with folding and uplift of their hangingwalls. Within the study area, rifting generated two major W-SW-dipping basement faults with several kilometres of normal offset. The larger Coffee Soil Fault delineate the eastern boundary of the rift basins. Within its hangingwall, a broad zone is characterised by inversion-related uplift and deformation. Along the fault, buttressed growth folds in the immediate hangingwall indicate thick-skinned inversion, i.e. coupled deformation between the basement and cover units. The opposite margin of the inverted zones follows the westwards pinch-out of the Zechstein salt. Here, thin-skinned folds and faults sole out into Zechstein units on the half-graben dip slopes. The most pronounced inversion occurred directly above and in extension of salt ridges and –rollers that localized shortening in the cover above. With no apparent links to underlying basement faults, we balance thin-skinned shortening to the sub-salt basement via a triangle-zone concept. This implies that thin Zechstein units on the half-graben dip slopes formed thrust detachments during inversion, and that basement shortening was mainly accommodated by reactivation of the major rift faults further east. Ductile deformation at seismic scales accounts for thin-skinned shortening of the cover units where such a detachment did not develop. We discuss the related mechanisms. The documented structural styles are similar to those found in other inverted basins in the region, and to those produced from physical-model experiments. Our results indicate that Zechstein units imposed a strong control on structural style and kinematics during basin inversion in large parts of the Danish Central Graben. We emphasize that even thin evaporite units may act as detachments during tectonic extension and contraction if favourably orientated. Salt ridges and diapiric structures can localise shortening and generate thin-skinned faults and folds in the cover above. In mildly inverted rifts, extensive mobile salt may mask the effects of basin inversion if shortening is accommodated by salt structures without the formation of clearly defined inversion structures at the surface or significant uplift.

https://doi.org/10.5194/se-2020-127
Preprint. Discussion started: 27 August 2020
© Author(s) 2020. CC BY 4.0 License.


1 Introduction

1.1 Basin inversion and the role of mobile evaporites

We define basin inversion as the shortening of previously extensional basins due to compression or transpression (cf. Cooper et al., 1989; Turner and Williams, 2004). From here, our use of the term "inversion" refers to basin inversion, unless specifically stated otherwise. It is recognizable from the structures that accommodate shortening and uplift of the basin packages: reverse reactivation of pre-existing normal faults or fault trends, i.e. fault inversion, and the development of shortcut thrusts and folds (e.g. Williams et al., 1989; Turner and Williams, 2004). Basin inversion is a fundamental process in the tectonic evolution of sedimentary basins. It may play an important role in the formation of hydrocarbon traps, although it can also have negative effects on the prospectivity of a basin (Turner and Williams, 2004). Many authors have reviewed the concept of basin inversion and the criteria for recognizing the resulting structures (see e.g. Cooper et al., 1989; Coward et al., 1991; Eisenstadt and Withjack, 1995; Coward, 1996; Kockel, 2003). Mild inversion refers to a small magnitude of shortening relative to the magnitude of earlier extension (Cooper et al., 1989). In recent years, the increased prevalence of borehole-constrained 3D seismic data of high quality has improved our understanding of inversion structures and their development, especially in basins that are only mildly inverted (e.g. Jackson and Larsen, 2008; Grimaldi and Dorobek, 2011; Jackson et al., 2013). Mild inversion is advantageous to such studies because pre-existing structures are still well resolved, making their role during inversion easier to delineate (Jackson et al., 2013).

Several physical-model studies have illustrated the structural styles and development of inversion structures (e.g. Koopman et al., 1987; McClay, 1989; Eisenstadt and Withjack, 1995; McClay, 1995; Brun and Nalpas, 1996; Bonini et al. 2012; Jagger and McClay, 2018), as well as how initial three-dimensional geometries of normal faults affect the development of inversion structures (e.g. Yamada and McClay, 2004). Depending on the reactivation of basement faults below the basin fill, the effects of inversion may vary a great deal between different parts of the extensional basin. Basement faults are more prone to reactivate in a reverse sense with gentle dip angles, oblique angles between their strike and the direction of shortening, low frictional resistances along fault planes, and high connectivity to fluids expelled from juxtaposed rocks (Bonini et al., 2012). Forced folding and short-cut structures tend to occur where the strikes of inherited extensional structures are approximately orthogonal to the direction of maximum compressive stresses, and where steeply dipping normal faults bound the basin (Letouzey, 1990). If instead, the incidence is oblique, a strike-slip component is induced that allows for reactivation of steeply dipping faults (Letouzey, 1990; Letouzey et al., 1990).

Additionally, workers have utilized physical models to investigate the structures formed by extension (e.g. Withjack and Callaway, 2000; Ferrer et al., 2017) and inversion of rift basins containing weak evaporite sequences (e.g. Nalpas et al., 1995; Brun and Nalpas, 1996; Bonini et al., 2012; Roma et al. 2018a; 2018b; Ferrer et al., 2017). These have shown that mobile evaporites can play a major role in the structural development of basins during both extension and inversion, due to their ability to decouple deformation (partially or fully) in the substrata and overburden. The model studies of Letouzey et al. (1995) showed that major controlling factors on the localization of reverse faulting and folding in inverted graben include pre-existing

https://doi.org/10.5194/se-2020-127
Preprint. Discussion started: 27 August 2020
© Author(s) 2020. CC BY 4.0 License.


extensional structures, salt thickness, and the distribution of older evaporite structures. Following salt deposition, salt ridges tend to form when extension causes salt to flow up-slope toward the crests of rotated footwall blocks (Vendeville, 1987; Vendeville and Jackson 1992a, 1992b; Nalpas and Brun, 1993). During subsequent contraction and inversion, folding and reverse faulting or thrusting will often initiate above salt ridges with favourable orientations, where the overburden is thinned and possibly faulted. This occurs even when there is no direct link to basement faults (Letouzey et al., 1995; see also Brun and Nalpas, 1996).

1.2 Study aims

Along with mobile-salt diapirism, basin inversion is responsible for a significant number of structural traps for hydrocarbon reservoirs in Cretaceous Chalks in the Danish Central Graben (Megson, 1992; Vejbæk and Andersen, 2002). The deformational histories and geometries of these reservoir strata are intimately related to basin inversion that occurred mainly in the Late Cretaceous, when they were buried only at shallow depths or still being deposited (Vejbæk and Andersen, 1987; Cartwright, 1989; Vejbæk and Andersen, 2002). Duffy et al. (2013) analysed the controls of mobile evaporites on the structural development during Triassic and Jurassic rifting in a smaller part of the Danish Central Graben (from here: DCG; Fig. 1). Their work highlights the DCG as a well-suited area for studying the structural controls of deep evaporites as the thickness of the Zechstein units here range from near zero in some areas to thousands of meters in salt structures. In addition, the combination of a mild yet considerable degree of inversion and the well-preserved extensional fabric provides an excellent opportunity to link the kinematics of inversion structures formed near the surface to deeper inherited structures and evaporites. This is the focus of the present study. We provide an updated kinematic analysis of a portion of the DCG (Fig. 1) in order to explain the role of mobile evaporites and salt tectonics during Late Cretaceous-Danian basin inversion, and the relationship between deformation in the sub-salt basement and supra-salt overburden. Since Vejbæk and Andersen (1987; 2002), and Cartwright (1989) performed the only dedicated investigations into basin inversion across the DCG, a wealth of knowledge has surfaced on extensional and contractional deformation of basins containing mobile evaporites (e.g. Vendeville and Jackson, 1992a; 1992b; Letouzey et al., 1995; Stewart and Clark, 1999; Withjack and Callaway, 2000; Bonini et al., 2012; Stewart, 2014). Our analysis incorporates these findings with our own results from seismic mapping and structural interpretation of a newly available high-quality 3D seismic data set from the DCG.

2 Geological setting

2.1 Paleozoic

The North Sea area has accommodated sediments since Cambrian times while experiencing both contractional, extensional and inversion-tectonic regimes (Ziegler, 1990; Vejbæk, 1997; Coward et al., 2003; Lassen and Thybo, 2012). The present outline of the North Sea Basin relates to an Early Permian thermal event and crustal extension (Vejbæk, 1997; Glennie et al., 2003). Early Permian rifting involved widespread volcanism, fault-block rotation and erosion of footwall crests (Stemmerik

https://doi.org/10.5194/se-2020-127
Preprint. Discussion started: 27 August 2020
© Author(s) 2020. CC BY 4.0 License.


et al., 2000; Mogensen and Korstgård, 2003; Coward et al., 2003; Glennie et al., 2003; Clausen et al., 2016). Post-rift thermal subsidence (sensu McKenzie, 1978) followed and formed the extensive Northern- and Southern Permian Basins separated by a c. E-W-striking basement high, which would later separate into the Mid North Sea- and Ringkøbing-Fyn Highs (Vejbæk, 1990; 1997; Sørensen 1986). In Late Permian times, the evaporites of the prominent Zechstein Group were deposited in these basins (Fig. 2a). These units pinch out towards the basin limits where marginal facies dominate while large volumes of halite formed in the basin centres (Stemmerik et al., 2000; Glennie et al., 2003). Inherited regional topography largely controlled the extent of the evaporites although rifting generated fault-controlled subsidence in e.g. the Central Graben and Horn Graben areas, which allowed thicker packages to accumulate (Clausen and Korstgård, 1993b; Korstgård et al. 1993). Due to later halokinesis, it is unknown whether faulting occurred during or prior to evaporite deposition (e.g. Duffy et al., 2003).

2.2 Triassic and Jurassic

Triassic rifting in the central and southern North Sea area generated c. N-S-striking faults as part of the development of the Central Graben and Horn Graben (Fig. 2b; Coward et al., 2003). The Mid North Sea and Ringkøbing-Fyn Highs highly influenced Triassic sedimentation as evident from lithological differences in the two basins. Continental clastics with local and thin evaporite beds dominated to the south (Fig. 2b), while occasional marine transgressions from the Tethys introduced marine conditions and flooded the Mid North Sea High. The most northward extent of these marine transgressions occurred in the eastern most part of the North Sea Basin (Berthelsen, 1980; Michelsen and Clausen, 2002). The Triassic sediments in the Danish Central Graben show a close relation to the area south of the Mid North Sea- and Ringkøbing Fyn Highs (Michelsen and Clausen, 2002). At this time, halokinesis involving Zechstein units initiated, and the differential subsidence due to halokinesis possibly controlled the distribution of fluvial sediments (Goldsmith et al, 2003; McKie et al., 2010; Jarsve et al., 2014).

The Jurassic was dominated by intense rifting, which highly influenced the Moray Firth, the Viking Graben and the Central Graben (Fig. 2c). Thermal doming at the triple junction initiated in Early Jurassic times and erosion of older deposits generated the widespread and easily recognizable Mid Cimmerian Unconformity (Coward et al., 2003). Intense Late Jurassic rifting occurred over two main phases. The first reactivated N-S-striking normal faults during E-W-directed extension. In the Danish Central Graben, this generated mainly eastward-dipping halfgrabens (Roberts et al. 1990). The second phase formed NNW-SSE striking faults that connected the older faults. This combination caused a rather complex fault pattern in the Danish Central Graben. Thick syn-rift mudstone deposits of especially the Farsund Fm. provide good source rocks locally (Michelsen et al., 2003).

2.3 Cretaceous and Cenozoic

Deposition of marine shales characterize the Early Cretaceous, while faulting gradually ceased in the Central North Sea area (Fig. 2d); Coward et al., 2003) and post-rift thermal subsidence formed accommodation (Sclater and Christie, 1980). Extensive deposition of pelagic shelf carbonates followed in Late Cretaceous times, forming the Chalk Group, while siliciclastic units

https://doi.org/10.5194/se-2020-127
Preprint. Discussion started: 27 August 2020
© Author(s) 2020. CC BY 4.0 License.


were restricted to the basin margins (Fig. 2e; Ziegler, 1990; Surlyk et al., 2003). Widespread inversion tectonism in the Alpine Foreland caused uplift and erosion of former depocentres as well as redeposition of sediments in the southern and central North Sea area (also Kley, 2018). Inversion generated a significant number of structural traps for producing hydrocarbon reservoirs in e.g. the Danish- and Norwegian parts of the Central Graben (Damtoft et al., 1987). The Post-Danian Paleogene was dominated by siliciclastic deposition from the emergent areas surrounding the North Sea Basin, meaning that the deep basin, including the Central Trough above the Mesozoic rift system, gradually filled (Gołedowski et al. 2012, Anell et al., 2012). Inversion activity in the North Sea Basin continued although the activity migrated westwards relative to the areas affected in the Cretaceous and Paleogene (Ziegler, 1990; Kley, 2018).

Locally in the DCG, inversion movements may have initiated as early as in the Late Hauterivian (Vejbæk, 1986). Although punctuated by pulses of increased activity, inversion was continuous in the DCG throughout the Late Cretaceous and Danian (Vejbæk and Andersen, 1987; 2002). Around the beginning of the Campanian, it became a major influence on the basin morphology, forming a prominent unconformity above earlier rift depocentres (van Buchem et al., 2018). The relative uplift caused by inversion occurred on a background of post-rift thermal subsidence, meaning that erosion was limited in comparison to other inverted basins in the southern North Sea. Paleogene inversion phases followed but generated only a wide and gentle flexure above the rift (Vejbæk and Andersen, 2002; Clausen and Korstgård, 1993a; Clausen et al. 2012). Areas that experienced inversion in the Late Cretaceous and Paleogene are indicated on Fig. 1.

3 Data and methods

3.1 Data

A regional merge of reprocessed data from several 3D reflection-seismic surveys with a total area of c. 6000 km^2, was available for this study. This covers most of the Danish Central Graben area. For this study, we used a subcrop of this dataset with an area of c. 4000 km^2, covering parts of the Heno Plateau-, Tail End Graben- and Salt Dome Province areas (Fig. 1) within the Danish Central Graben. The dataset is Kirchhoff pre-stack depth-migrated, has a 12,5 m inline- (N-S direction) and crossline (E-W direction) spacing, and extends to a depth of 10 km. The vertical sampling rate is 4 ms, and the seismic wavelet is zero phase with European polarity. Therefore, in the seismic sections shown herein, a negative amplitude (trough) corresponds to a downward increase in acoustic impedance, i.e. a hard response. The velocity model applied for depth-imaging is verified with checkshot data and sonic data from wells.

Within the Chalk Group, the vertical seismic resolution is c. 25 m, i.e. the quarter of the wavelength of the dominant frequency. The signal quality is generally excellent, although it deteriorates close to and below large lateral discontinuities e.g. salt diapirs, large faults, and subvertical strata. We chose to analyse depth-converted seismic data in order to avoid structural misinterpretations of apparent deformation caused by velocity variations. A large number of wells were available for this study along with formation tops constrained from biostratigraphy.

https://doi.org/10.5194/se-2020-127
Preprint. Discussion started: 27 August 2020
© Author(s) 2020. CC BY 4.0 License.

Solid Earth Discussions

3.2 Methods

3.2.1 Seismic-stratigraphic analysis

The methods applied in this study follow common procedures applied in tectono-stratigraphic basin analyses from seismic data. Initially, relevant seismic surfaces were mapped (Fig. 3) along with prominent deformational structures, i.e. faults, folds and salt structures. Our seismic surfaces from Top Pre-Zechstein to Top Chalk Group are equivalent to surfaces of the same names illustrated by van Buchem et al. (2018). The upper surfaces, Top Stronsey Group and Upper Oligocene Unconformity, are equivalent to those used by Clausen et al. (2012). Surfaces following continuous reflections of moderate to high amplitudes were favoured in order to make mapping across the study area easier with the aid of formation tops in wells. For mechano-stratigraphic purposes, we refer to all deposits above the Zechstein units as (supra-salt) cover, and everything below including non-crystalline deposits, as (sub-salt) basement (cf. Duffy et al., 2013).

Only few wells reach the basement in the study area, either on the Ringkøbing-Fyn High (crystalline rocks) or in the western part of the study area where Zechstein Group deposits are absent (Lower Permian Rotliegende deposits). In addition, Zechstein evaporites are only reached by wells atop mobile-salt structures. We therefore mapped the top and base of the Zechstein Group away from these structures with the aid of seismic-facies analysis (cf. Duffy et al., 2013). The Zechstein salt is recognizable due to its chaotic seismic facies with low-amplitude and discontinues reflections in contrast to the parallel and better-defined reflections of the deposits above and below.

Surface depth-structure maps were produced to investigate the current structural configuration, and in order to calculate isochore maps (vertical thickness) for the Zechstein Group (Upper Permian), Cromer Knoll Group (Lower Cretaceous), Chalk Group (Upper Cretaceous and Danian), and Paleogene excl. Danian. We then analysed the isochore maps in order to identify differential subsidence caused by faulting, folding or mobile-evaporite movements. This assumes that the observed differences in thickness are a proxy for subsidence variations due to these movements. However, differential compaction, water level and sedimentary processes and supply also affect subsidence to a significant degree (see e.g. Sclater and Christie, 1980; Bertram and Milton, 1989). Therefore, we integrated observations of stratal relationships to obtain a higher degree of certainty in the delineation of subsidence patterns and the reconstruction of past basin geometries.

We carried out analyses of the structural elements indicated by the isochore maps to have been active during the Cretaceous and Paleogene when basin inversion occurred. Based on observations of their geometries, magnitudes and age relationships, these analyses include qualitative descriptions of the kinematics and the mechanics involved in generating these structures. We describe their kinematic relationships with deeper structures, especially Zechstein salt and basement faults, in order to infer the deformation of the deeper basin due to inversion. We note that a detailed seismic-stratigraphic analysis of the syn-inversion (cf. Vejbæk and Andersen, 1987; 2002; Clausen and Korstgård, 1993a) units would greatly increase the temporal resolution of our kinematic analysis. This would provide a stronger basis for linking the kinematics of inversion and halokinesis in the area, but is beyond the scope of the present study.

https://doi.org/10.5194/se-2020-127
Preprint. Discussion started: 27 August 2020
© Author(s) 2020. CC BY 4.0 License.


3.2.2 Analysis of mobile-salt migration

In accordance with the assumptions and method of Duffy et al. (2013), we classify the Zechstein units as immobile in areas where their thickness is generally below 200 m and they are restricted to local topographical lows in the Top Pre-Zechstein surface (Duffy et al. used <100 ms TWT. This corresponds to 225 m with a seismic velocity of 4500 m/s). On this basis, we constructed a "mobile-salt pinch-out" to separate the present-day domains characterized by either immobile (thin) or potentially mobile Zechstein salt (thick).

Duffy et al. (2013) demonstrated that "tongues" of Zechstein units were initially present beyond the modern-day pinch-out of mobilized Zechstein east of the Gorm-Tyra Fault. These either dissolved or retreated southward into the larger mobile-salt structures. Similar movements may have taken place in the hangingwall of the Gorm-Tyra Fault and in the Tail End Graben, where salt could have migrated towards areas of lower pressure inversion. As mobile evaporites impose controls on deformation, the differences between the syn-inversion- and modern-day distributions of mobile Zechstein units could have significant implications for the kinematics of inversion. We have therefore included an analysis of the subsidence patterns of the Cromer Knoll Group (Early Cretaceous, pre-inversion) to aid in constraining the extent of the mobile Zechstein salt at the onset of inversion. Vejbæk (1986) indicated that halokinesis influenced the subsidence pattern during the Early Cretaceous, and it is possible that similar salt movements continued into the Late Cretaceous and modified some inversion structures. In our analyses, we have only considered the salt budget qualitatively, but the relatively small volumes of salt withdrawal inferred from local Cretaceous depocentres, we deem realistic considering the continued growth of several large salt structures into even Neogene times. In addition, dissolution of salt from diapirs may have removed some amounts trough time (Korstgård et al., 1993; Rank-Friend and Elders, 2004).

4 Results and interpretations

In this chapter, we present findings from our analysis of the seismic data. We first describe the structures and geometries of the sub-salt basement and the Zechstein Group along with the current areal distribution of potentially mobile and non-mobile Zechstein units. We then characterize the structural styles of inversion-related deformation during Late Cretaceous-Danian times and post-Danian times, respectively. Finally, we infer the distribution and movements of mobile Zechstein units during Early- and Late Cretaceous, and Paleogene times, as these may have implications for the contemporary kinematics.

4.1 Sub-salt structures and geometry

Two major rift faults occur in the study area: The Coffee Soil Fault and the Gorm-Tyra Fault. The overall structural architecture of the Pre-Cretaceous in the study area approximates that of a NW-SE-trending halfgraben bounded by the Coffee Soil Fault. This major structure constitutes the master rift fault along the northeastern boundary of the Central Graben throughout the Danish North Sea (Gowers and Sæbøe, 1985; Cartwright, 1991). In our study area, it consists of three linked normal-fault segments with different strike directions (Fig. 9b): segment 1 in the north and segment 3 in the south strike c. NNW-SSE while

https://doi.org/10.5194/se-2020-127
Preprint. Discussion started: 27 August 2020
© Author(s) 2020. CC BY 4.0 License.


the central segment 2 has a c. WNW-ESE strike. The fault is generally well imaged on the seismic data and is even traceable below the rift basin floor in some places. This reveals the planar shape of each segment along the Triassic-Jurassic units in the hangingwall, and relatively small dip angles (cf. Cartwright, 1991) of segments 1 and 3 are: c. 37° and c. 32° respectively. This contrasts the c. 50° dip angle of segment 2. The other major basement fault in the study area, the Gorm-Tyra fault is a west-dipping normal fault striking c. N-S (Fig. 9b). It extends from the intersection of segments 1 and 2 of the Coffee Soil Fault and through the southern edge of the study area and shows a consistent dip angle of c. 40°. Its throw at Top Pre-Zechstein level is generally c. 2 km along its length, and unlike the Coffee Soil Fault, it does not extend up through the Mesozoic syn-rift succession.

A large number of subsidiary normal faults offset the Top Pre-Zechstein with a significantly higher density in the western part of the study area (Heno Plateau) compared to east of the Gorm-Tyra Fault (Fig. 9b). Although they are often difficult to map with certainty due to limited data quality at depth, their strike trends are generally E-W to N-S, i.e. equivalent to those of the Coffee Soil Fault segments and the Gorm-Tyra Fault. We have observed no reverse faults at Top Pre-Zechstein level. Two broad anticlines striking WNW-ESE with relatively limited lengths occur near the confluence of segments 1 and 2 of the Coffee Soil Fault in the Tail End Graben and Poul Basin respectively.

In the hangingwalls of segment 1 of the Coffee Soil Fault the Gorm-Tyra Fault, the Top Pre-Zechstein dips significantly towards the faults, up to c. 20°. It reaches its deepest points of c. 9,5 km in the Tail End Graben, and nearly 9 km at the confluence of segments 1 and 2 of the Coffee Soil Fault and the Gorm-Tyra Fault. This equates to fault throws of more than 6 km, although this is a minimum estimate given that no pre- or syn-rift deposits are preserved in the footwall. To the east of the Gorm-Tyra Fault, the basin floor is generally closer to horizontal and does not steepen toward the Coffee Soil Fault, except in the immediate hangingwall of segment 2. The Poul Plateau at the confluence of segments 2 and 3, and the Mads High in the west constitute the two shallowest basement elements in the study area apart from the Ringkøbing-Fyn High.

Lower Permian Rotliegende units underlie the Top Pre-Zechstein in the western part of the study area, where Zechstein units are absent (Fig. 9c). No wells penetrate beyond the Triassic in the deeper parts of the DCG in the study area, meaning that the nature of the Pre-Zechstein basement is unknown here. Parallel reflections on both sides of the Gorm-Tyra Fault suggest that Paleozoic deposits may extend across much of the study area below the Zechstein salt.

4.2 Current distribution and geometry of Zechstein units

Zechstein units range in thickness from thin or below seismic resolution in the central part of the study area, to extreme local maxima in diapiric structures in the southern (Salt Dome Province) and very northwestern parts (Fig. 9e). Zechstein deposits are absent where the Top Pre-Zechstein is the shallowest i.e. on the Heno Plateau to the west (cf. Vigeland Ridge of Gowers and Sæbøe, 1985) and on the Ringkøbing-Fyn High. Only few significant faults offset the Top Zechstein surface within the larger basin (Fig. 9d). Along the western pinch-out of Zechstein deposits on the halfgraben dip-slopes, we have interpreted three reverse faults or thrusts that sole out into Zechstein units. The two largest occur along the Arne Ridge and Bo-Jens Ridge, where they reach Cretaceous levels (Fig. 4-6). The third occurs in relation to folded overburden strata at the Edna structure

https://doi.org/10.5194/se-2020-127
Preprint. Discussion started: 27 August 2020
© Author(s) 2020. CC BY 4.0 License.


(Fig. 6). Also detaching into the Zechstein, a prominent normal-fault trend links the Gorm-, Skjold- and Dan structures (Fig. 9d). The northern part of the Gorm-Tyra Fault offsets the thin package of Zechstein found here, while to the south, the Top Zechstein drapes the fault, which is only expressed as a large monocline at shallower levels.

The constructed mobile-salt pinch-out effectively marks the boundary of the Salt Dome Province in the south, while only a small area in the north contains potentially mobile Zechstein (Fig. 9f). In the Poul Basin area, only pockets of Zechstein reaching thicknesses >200 m occur (Fig. 9e). These pockets fill topographical lows in the Top Pre-Zechstein surface that exhibit erosional rather than structural characteristics (cf. Duffy et al., 2013). The Salt Dome Province and the northern Tail End Graben area are characterized by large salt pillows, -ridges and -rollers with extreme thicknesses of Zechstein (>400 m) within and immediately around them (Fig. 9f). In the Salt Dome Province, the areas of thin or absent Zechstein between these structures show typical signs of salt deflation and –withdrawal. The Triassic-Jurassic cover is folded into synclines that trend parallel to the salt structures. Units of mainly Late-Jurassic age occur within the syncline centres, onlapping their flanks (e.g. Fig. 7). We therefore infer that Zechstein salt was initially deposited relatively evenly across the Salt Dome Province, including the area west of the Gorm-Tyra Fault, before it was mobilized due to rifting and eventually left the overburden welded to the substrate (cf. Rank-Friend and Elders, 2004; Duffy et al., 2013).

Several prominent salt structures of varying maturities populate the current-day mobile-salt domains (Fig. 9f). Salt stocks of different sizes populate the Salt Dome Province, including the Edna-, Rolf-, Dagmar-, John- and Skjold structures. These all penetrate Cretaceous strata (Fig. 11c), with the John structure reaching the shallowest level around 0,5 km below sea level (water depth less than 50 m). Other intrusive diapirs (sensu Jackson and Talbot, 1986) include the Gorm-, South-Arne-, and Dan structures. At a glance, their 3D shapes are more elongate and complex than those of the stocks, and although their influence is evident at Base-Cretaceous levels (Fig. 11e), they have not penetrated into Cretaceous strata. The Dan structure is remarkable, as Zechstein salt has delaminated the Triassic succession laterally along weak evaporite horizons to form wings or salt wedges (sensu Kockel, 2003) that extend laterally for several kilometres (Rank-Friend and Elders, 2004). A handful of concordant (sensu Jackson and Talbot, 1986) salt structures with more than 1000 vertical meters of salt are present in the modern-day mobile-salt domains. One of them may be considered part of the Dagmar structure, whereas the four others are isolated structures. These include the named structures Kraka (c. 1800 vertical meters of salt) and Lola, as well as a previously unnamed structure near the Jens-1 well, which we refer to as the Jens Pillow (Fig. 9f). A network of smaller salt ridges and –rollers connect the larger structures in the southern part of the study area. The elongated axes of all salt structures appear to align with the underlying basement fault trends. This is especially evident to the east of the Gorm-Tyra fault. In the northeastern part of the Tail-End Graben, a local Zechstein thickness maximum may represent a considerable volume of trapped salt relative to its depth, although the data are noisy in this area. Korstgård et al. (1993) interpreted trapped Zechstein units to be present in the immediate hangingwall of the Coffee Soil Fault just north of our study area, which lends supports to this interpretation.

Beyond the mobile-salt pinch-out, we infer the presence of mechanically weak Zechstein units from the observation that the Top Zechstein reflection (base of the Triassic carapace) is smooth and continuous, while the Top Pre-Zechstein is more uneven and discontinuous. In parts of the Tail End Graben, this contrast in morphology is not apparent (marked area on Fig. 9c).

https://doi.org/10.5194/se-2020-127
Preprint. Discussion started: 27 August 2020
© Author(s) 2020. CC BY 4.0 License.


Zechstein units may be absent here or only present in thicknesses near the limit of seismic resolution. Due to low data quality at depth in this area, the exact position of the western pinch-out of the Zechstein units and their thickness are unclear along the southern Arne-Elin trend (Fig. 9f).

4.3 Structural styles of Late Cretaceous-Danian inversion

Our following descriptions of Late Cretaceous-Danian inversion structures agrees overall with those of Vejbæk and Andersen (1987; 2002) and Cartwright (1989). Unlike these workers, we do not take into account the diachroneous and gradual development of many of the structures apart from before and after the end of Danian times. Instead, we pay greater attention to the structural connections between the upper inversion structures and the Zechstein units and Pre-Zechstein basement below. Across our study area, Late Cretaceous-Danian inversion is evident from open growth folds and reverse faults along the outer margins of the uplifted basins (Figs. 4-8). Relative uplift is evident especially from Lower Cretaceous units (Cromer Knoll Group) that sit at shallower levels compared to adjacent areas with no preserved Lower Cretaceous units. Except along the Arne Ridge, folding apparently accommodated significantly more shortening and uplift than reverse faulting. The distribution of major growth folds, characterised by onlapping Chalk Group strata, is evident from the isochore map of the syn-inversion Chalk Group (Figs. 11e-f). Thinning of Chalk Group units and truncations are also evident on the fold crests. Major folds generated by inversion are mostly recognizable as asymmetric anticlines and monoclines with steep forelimbs facing the marginal troughs and more gently sloping backlimbs (cf. e.g. Koopman et al., 1987; Badley et al., 1989). In the most extreme cases (e.g. Bo-Jens Ridge), these inversion ridges express a relief of c. 1000 m relative to the adjacent marginal basins at Base Chalk Group level. We also interpreted inversion-related synclines as outlined further below. Aside from atop inversion ridges and salt diapirs, the only place with Chalk Group units thinner than 200 m is the Mads High, where it sits directly on Pre-Zechstein units.

The faults related to inversion are mostly inverted extensional faults that extended slightly upwards during shortening, giving them the typical expression with reverse offsets only in their highest parts (e.g. Fig. 5). Few reverse faults and thrusts appear to have formed as shortcuts. Relative to folding, reverse faulting is significantly less prominent at Base Chalk Group level and in the syn-inversion strata above (Fig. 11b), as seen from e.g. the Bo-Jens Ridge and the Adda Ridge (Fig. 6). Much of the then-shallow reverse faulting only reached into the pre-inversion Lower Cretaceous units, while fault-tip folding probably accounted for the strain at seafloor level. Faults offsetting the Base Cretaceous Unconformity (Fig. 10b) reveal that reverse reactivation of normal faults was selective as not all faults with similar strike directions inverted. All inversion folds and faults show strike directions within WNW-ESE to N-S, which concurs the structural trends of the sub-salt basement. From our observations, we outlined the margins of the inverted zones (indicated on Fig. 11f) outside of which no significant signs of Late Cretaceous inversion are apparent. The zone within the margins spans the entire southern study area and becomes narrower towards the north.

A number of smaller extensional growth faults occur locally in the Chalk Group, which formed and were active in Late Cretaceous times, possibly during inversion. Some likely formed due to differential compaction across large but inactive

https://doi.org/10.5194/se-2020-127
Preprint. Discussion started: 27 August 2020
© Author(s) 2020. CC BY 4.0 License.


extensional faults (Fig. 11b). Others populate the crests of inversion ridges (e.g. Bo-Jens Ridge, Fig. 6, and Gorm-Lola Ridge, Fig. 7) or appear near the inversion margins (Figs. 11b and 11d). Local extension, e.g. due to outer-arc stretching or slope instabilities, could have generated these faults (see e.g. Back et al., 2011).

Post-Danian inversion is evident from the wide and gentle Tyra-Igor Ridge, which is expressed in the Top Chalk Group topography (Fig. 11d; cf. Vejbæk and Andersen, 1987; 2002). Compared to the structural styles of Late-Cretaceous inversion, this is markedly different. Instead of prominent folds along the margins of the uplifted areas, a broad flexure centred above the Late Jurassic rift depocentres characterizes this inversion. In addition, no related reactivation of extensional faults in the cover units is evident.

4.3.1 Eastern inversion margin

The eastern margin of the inverted zones follow the upper trace of the Coffee Soil Fault, although slightly basinwards along segment 1 (Fig. 11f). Striking parallel to segments 2 and 3, the prominent Adda- and Igor-Emma Ridges display classical traits of buttressed folds situated directly above inverted rift-bounding faults (Figs. 6 and 8). The axial traces of these folds are traceable c. 1-2 km into the deeper pre-inversion units. Below this, the Jurassic and Triassic units show no apparent reverse drag along the surface of the Coffee Soil Fault. Noticeably, a possible Zechstein salt intrusion occurs along the plane of the Coffee Soil Fault below the southern part of the Igor-Emma Ridge (Fig. 8). The top of this body coincides with the base of the anticline axial trace, indicating a kinematic connection during inversion. The basin units above the Poul Plateau are not significantly uplifted and show no buttress folds at Cretaceous levels, even though reverse offsets in the upper part of the Coffee Soil Fault segments are evident. To the southwest the extensive Alma Slope is seemingly unaffected by distinct folds or reverse faults.

Only a narrow but prominent anticline overlie the southernmost part of segment 1 of the Coffee Soil Fault northwest of Adda Ridge. Unfortunately, this structure is mostly obscured by the gap in the seismic data here (Fig. 11f). Following the Coffee Soil Fault northwest, no significant inversion structures occur directly above it. Instead, the Gulnare Basin and Iris-Adda Slope provide a more gradual transition from non-inverted footwall to inverted basin. Syn-inversion faults and folds populate this area; most noticeably, a large monocline is traceable many kilometres into the Tail End Graben fill (Fig. 5).

4.3.2 Western inversion margin

Going north to south, the western margin of the inverted zones separates the Eg-Ravn Basin from the Arne Ridge and Bo-Jens Ridge after which it follows a group of smaller ridges connecting the Edna and Rolf salt structures. The Arne Ridge formed due to inversion of the Arne-Elin Graben, which was a fault-bounded depocentre in Early Cretaceous times (Vejbæk and Andersen, 1987; see Figs. 10c-d). It represents the most pronounced inversion structure in the northern part of our study area (Fig. 4). In the northwest, it connects to the South-Arne salt structure and in the southeast, the Bo-Jens Ridge. Although it seems to follow a fault trend in the Top Pre-Zechstein surface, these are poorly visualised in the seismic data and their dip directions uncertain. The extent of the Zechstein salt southeast below the Arne Ridge is also uncertain. It may extend along

https://doi.org/10.5194/se-2020-127
Preprint. Discussion started: 27 August 2020
© Author(s) 2020. CC BY 4.0 License.


most of the structure as a small salt ridge at which the southwest-verging thrusts and reverse faults sole out along the Zechstein salt (Fig. 4-5).

The Bo-Jens Ridge strikes north to south and expresses significantly less faulting relative to the Arne idge (Fig. 6). This coincides with the thin Lower Cretaceous units in the structure (Figs. 10c-d), indicating that this was not a pre-existing depocentre. The anticlinal fold is the largest in the north and plunges towards the south where it is more monoclinal and eventually undistinguishable from folding related to the Jens Pillow. It follows a west-dipping normal fault in the basement, which is either absent or obscured below the northern part. The associated reverse fault below the fold soles out into Zechstein units along the crest of a salt roller (sensu Jackson and Talbot, 1986) below the southern part of the structure. This roller forms the most northern point of the southern mobile-salt domain. Notably, this reverse fault records the deepest net reverse offset on a fault in the study area at the Near Top Callovian surface. Judging from the east-west change in thickness of Upper Jurassic units, the fault probably formed during rifting before it was inverted in the Late Cretaceous. Slight folding of the cover units in the adjacent part of the Eg-Ravn Basin reveals the effect of inversion here.

A group of narrow anticlinal folds cored by mobile Zechstein units emerge from the southern Eg-Ravn basin. These record shortening and relative uplift on their east-facing flanks while only a single small breakthrust emerges from the detachment (Fig. 6). The folds connect the Edna- and Rolf salt structures before continuing southwards out of the study area.

4.3.3 Salt Dome Province

The wide zone between the inversion margins in the southern part of our study area, is dominated by large mobile-salt structures as described above. There are few structures that directly indicate shortening in the cover units, and none below the salt. Two thin Triassic evaporite units act as secondary detachment horizons for Mesozoic faults above the Zechstein (Fig. 8): the Muschelkalk Halite and the Röt Halite, which Michelsen and Clausen (2002) documented from U-1 well logs. According to them, the Main Röt Halite Member is c. 50 m and the Muschelkalk Halite Member c. 60 m thick in the U-1 well.

Above the footwall of the Gorm-Tyra Fault, the Gorm-Lola Ridge is a prominent and complex structure cored by the Gorm diapir, the Lola pillow and their connecting salt ridge (Fig. 7). Stratal thinning indicates that it formed in the Late Jurassic and remained a topographical high well into the Late Cretaceous. Onlaps in the Upper Cretaceous and a reverse fault soling out into the Muschelkalk Halite, indicate shortening related to inversion. WSW-ESE-striking faults sole out into the Muschelkalk Halite above the Kraka pillow as well (Fig. 8). Only the southernmost of these faults records both Late Jurassic extension and later inversion. Although not apparent from Cretaceous levels, this reverse fault offset at the base of the Upper Jurassic can be traced westwards where it connects to the reverse fault below the Gorm-Lola Ridge. Late Cretaceous folding above the Dan structure (Fig. 8) may be a result of shortening or halokinesis. Nearby along the same seismic section, a group of extensional faults sole out into the deeper Röt Halite. No faults soling out into this horizon seem to have activated during inversion in the area.

https://doi.org/10.5194/se-2020-127
Preprint. Discussion started: 27 August 2020
© Author(s) 2020. CC BY 4.0 License.


4.4 Mobile-salt distribution and movements during the Cretaceous

The volume of the Lower Cretaceous units in the study area is small compared to that of Upper Jurassic units. Locally pronounced thickness maxima indicate areas of increased subsidence, namely in the Arne-Elin Graben, Iris-, Gulnare- and Roar Basins (Fig. 10d). Of these, only the Gulnare basin sits adjacent to the Coffee Soil Fault, and only the Arne-Elin Graben shows patterns of fault-controlled subsidence. Along segments 2 and 3 of the Coffee Soil Fault, the Lower Cretaceous thins and onlaps towards the fault trace, suggesting no syn-depositional activity of the fault. The depocentre of the Roar Basin shows characteristic onlaps onto the flanks of a large syncline in the units below along with a lack of remaining Zechstein units below these, indicating that it formed as salt retreated towards the neighbouring salt structures (cf. Vejbæk, 1986). The Gulnare- and Iris basins may also have seen increased subsidence due to on-going salt retreat towards the west and northwest after Late Jurassic rifting ceased (see also Korstgård et al., 1993).

Significant Early Cretaceous faulting occurred in the Arne-Elin Graben, focusing subsidence along its northeastern flank, which is defined by a southwest-dipping fault (Fig. 10d). Thinned units indicate the presence of the South-Arne structure to the northwest. As mentioned, remnants of a salt ridge may extend southeast below the Arne-Elin Graben. Salt retreat from this ridge towards the South-Arne structure could have focused and enhanced the tectonically induced subsidence of the narrow graben, which commenced in the Late Jurassic (Møller and Rasmussen, 2003). Cartwright (1989) went as far as to argue that the normal faults offsetting the Base Cretaceous Unconformity across the DCG most likely resulted from differential compaction of Late Jurassic units or the withdrawal of Zechstein salt, rather than basement movements due to regional rifting. Continued halokinesis in the Late Cretaceous is evident from the Chalk Group isochore map (Figs. 11e-f). In the north, the South-Arne structure stand more out than from the Cromer Knoll Group thickness variations (Figs. 10c-d), suggesting that it grew upwards in combination with inversion of the Arne-Elin Graben. Distinct synclines occur parallel to inversion anticlines and monoclines above the Tail End Graben and in the southern study area (Figs. 4, 6, and 7), indicating that the lower part of the Chalk Group was folded and subsequently onlapped. The synclines widen with depth in the units below until they reach the basin floor. We interpret these structures as the results of combined salt retreat and buckling due to inversion. The apparent southwards migration of the Early Cretaceous Roar Basin depocentre indicates the progressive welding of the Triassic units to the basin floor as mobile salt migrates south along the Gorm-Tyra Fault. Additionally, Late Cretaceous rim synclines have formed adjacent to the Dagmar and Skjold structures due to diapiric growth. As indicated on the Top Chalk Group surface (Fig. 11c), the South-Arne- and Edna structures continued their growth into Cenozoic times, which led to thinning above them. Thickening around the Dagmar- and, to some degree, the John structures point towards continued growth as well.

5 Discussion

In this chapter, we compile and discuss our results and interpretations in relation to:

1. The controls of evaporites on inversion structures in the study area and mildly inverted basins in general
2. The kinematics of basement shortening and basement-fault inversion

https://doi.org/10.5194/se-2020-127
Preprint. Discussion started: 27 August 2020
© Author(s) 2020. CC BY 4.0 License.


3. The magnitude and direction of shortening during inversion
4. The mechanisms responsible for ductile deformation styles in the cover units

Our observations and interpretations most important to the following discussion include:

- All basement faults record net normal offsets at Top Pre-Zechstein level (Fig. 9b), and we have not interpreted contractional structures with certainty. Only two anticlinal folds in the deepest part of the footwall of the Coffee Soil Fault candidate as such.
- Zechstein units extend across most of the deeper basin floor in the hangingwalls of the Coffee Soil Fault and the Gorm-Tyra Fault (Fig. 9c). They pinch out on the western halfgraben dip-slopes and along the Coffee Soil Fault. Mobile-salt structures are restricted to the Salt Dome Province and the northern mobile-salt domain, although salt ridges extend towards the centre of the study area below the Bo-Jens Ridge and possibly the Arne Ridge (Fig. 9d).
- Prominent folding and selective fault reactivation, which characterise Late Cretaceous-Danian basin inversion, affected the deeper syn-rift units in several places (e.g. Fig. 5). Along the western margin of the inverted zones, thin-skinned inversion structures dominate with reverse faults soling out into Zechstein units (Fig. 11f). The major inversion folds follow not only basement fault trends, but also overlie salt ridges (Fig. 12). Along the eastern margin, thick-skinned inversion ridges follow the upper trace of the Coffee Soil Fault segments, except along segment 1 where the inverted basin rises only gradually into the hangingwall (Fig. 4). In the Salt Dome Province, some inverted faults sole out into the thin Triassic Muschelkalk halite below the Gorm-Lola Ridge and above the Kraka salt pillow (Fig. 8).
- During the Early Cretaceous, salt retreat formed the Roar Basin depocentre, and possibly contributed to the development of the Arne-Elin Graben, the Iris Basin and the Gulnare Basin in combination with extensional tectonism (Fig. 12). Salt flow into or away from an area respectively, may have enhanced anticlinal or synclinal folding of the cover above. These interpretations imply that mobile Zechstein salt was initially present in significant amounts beyond the modern-day mobile-salt pinch-out in the area.

5.1 Evaporite controls on inversion structures

In addition to the correlation between the major Late Jurassic rift depocentres and the Late Cretaceous-Danian inversion zones (Vejbæk and Andersen, 1987; 2002; Cartwright, 1989), there is a strong correlation between the extent of the Zechstein units and salt structures, and the areas affected by Late Cretaceous-Danian basin inversion along the western inversion margin (Fig. 12). In the southern part of the study area where mobile Zechstein salt is abundant, the outer margins sit far apart. The more prominent inversion folds are limited to the margins, while the effects of shortening are relatively subdued in between. In the northern part, the inversion zone is narrower, mimicking the extent of Zechstein units below, and much more pronounced across its width (Fig. 5). Thick-skinned inversion structures along segments 2 and 3 of the Coffee Soil Fault show typical geometries related to inversion of master rift faults.

https://doi.org/10.5194/se-2020-127
Preprint. Discussion started: 27 August 2020
© Author(s) 2020. CC BY 4.0 License.


The physical models of Letouzey et al. (1995) illustrate kinematics that are directly applicable to the geometries observed along the western inversion margin. As known from fold and thrust belts, evaporite pinch-outs impose a major control on deformation geometries, whether they are of structural or depositional origin. This is because the pinch-outs limit the possible extent of detachment horizons and thus localize the formation of contractional structures in the sedimentary overburden. Pre-existing salt structures, e.g. ridges, pillows and reactive diapirs, also localize folding, reverse faulting and thrusting in the cover during inversion (Letouzey at al., 1995). According to our kinematic interpretation (Fig. 13a), the Zechstein detachment and salt ridges along the western margin (Fig. 12) decoupled the thin-skinned inversion structures from the basement faults below. The only potential exception to this pattern is below the confluence of the Arne- and Bo-Jens Ridges. Due to the limited visibility here and possible absence of the Zechstein detachment, thick-skinned faults may be present. To the northwest along the base of the Arne-Elin Graben and to the south along the base of the Bo-Jens Ridge, small salt ridges localized shortening, and thin-skinned faulting and folding formed the prominent inversion structures in the thinned and weakened cover above.

These kinematics imply that the cover was sliding westwards and up-dip on top of the Zechstein detachment away from the Coffee Soil Fault segment 1 and the Gorm-Tyra Fault due to reverse slip on these faults. It seems curious then, that few signs of thick-skinned inversion are seen directly above them. To explain why these are missing, we apply a conceptual model described by Stewart (2014). This describes the development of a rift halfgraben with a weak basal detachment expressing thin-skinned inversion up-dip in the hangingwall opposite to the basement fault, above which no signs of inversion occur. This geometry is seen in several inverted basins in the North Sea and elsewhere (Stewart, 2014). During pre-inversion extension, a thick-skinned master fault (Coffee Soil Fault segment 1 / Gorm-Tyra Fault) initially offsets both basement and cover. Domino-block rotation gradually reduce the dip angles of the master fault while increasing the detachment dip angle towards it. Friction eventually inhibits slip on the upper part of the master fault, causing a fault weld to form as the cover rolls onto the footwall block during continued extension. An extensional triangle zone is now apparent in the hangingwall basement as continued slip is now accommodated by the basal detachment that dips towards the master fault. Higher on the dip-slope, thin-skinned normal faults (at Arne-Elin Graben and Bo-Jens Ridge) now form in the cover to balance the extension on the basement master fault, while a symmetrical syncline becomes apparent directly above the triangle zone. During the following contraction, the triangle zone reactivates causing backthrusting through the detachment, generating up-dip thin-skinned inversion structures (at Arne Ridge and Bo-Jens Ridge). Figure 13a illustrates this concept in the kinematic development of the Bo-Jens Ridge as suggested from our interpretation. The rate and magnitude of displacement during rifting and inversion must have been relatively low to allow the gliding of the cover units on the thin Zechstein detachments during shortening. The areal extent of slip on the Zechstein detachments remain unknown. It would have been restricted, depending on the presence of Zechstein units around the confluence of Bo-Jens Ridge and Arne Ridge. Here, ductile pure-shear deformation (at seismic scale) of the syn-rift cover may account for some thin-skinned shortening as well (see below).

We propose that the salt ridges and -rollers along the western inversion margin formed along the pinch-out of the Zechstein units, as mobile salt flowed up-dip along the basin floor during rifting and overburden loading (cf. Korstgård et al., 1993). Late

https://doi.org/10.5194/se-2020-127
Preprint. Discussion started: 27 August 2020
© Author(s) 2020. CC BY 4.0 License.


Jurassic onlapping onto the salt ridge cover below the Bo-Jens Ridge supports this (Fig. 6). In the case of the Arne-Elin Graben, passive diapirism likely occurred in the Early Cretaceous.

Even when salt is present in its hangingwall, thick-skinned inversion styles occur along segment 3 of the Coffee Soil Fault (section 5). This is comparable to the observations of Jackson et al. (2013) from the Egersund Basin (offshore Norway). We suggest that the relatively horizontal basin floor in the Salt Dome Province does not provide a favourable geometry for fault detachments during inversion. Indeed, the main inverted faults atop the Kraka structure (Fig. 8) and the reverse fault of the Gorm-Lola Ridge (Fig. 7) both sole out into thin Triassic detachments with significant dip angles. Along with the interpretations of thin-skinned structures mentioned above, this demonstrates that even thin evaporite layers and apparent welds (sensu e.g. Jackson et al., 2014) were activated as detachments during inversion if their orientations were favourable, e.g. along the sloping floor of a halfgraben. Additionally, if mobile evaporites are present in sufficient amounts to form ridges or reactive diapirs, thin-skinned folds and faults in the overburden will initiate from these or from detachment horizons above their flanks. Figure 13b illustrates the pre-inversion Kraka structure and the reactivation of thin-skinned faults soling out into Triassic evaporites on its flank in the Late Cretaceous.

In central areas with potentially mobile Zechstein units at the time of inversion, the effects of shortening are not as evident as along the inversion margins. As mentioned, we interpret the narrow Late Cretaceous synclines as resulting from an interplay of inversion-related buckling and salt retreat. Besides the subtle reactivation along the crests of the Kraka structure and Gorm-Lola Ridge, we are able to infer basin inversion only from the thick-skinned Igor-Emma Ridge in the southern part of the study area. Still, the mobile salt structures striking WNW-ESE to N-S are likely to have taken up at least a slight amount of shortening via lateral squeezing of the salt bodies. This would have elongated the structures orthogonally to the shortening direction, and tightened the cover folds above, explaining e.g. the slightly anticlinal expression of the Dan structure on the Chalk Group isochore map (Fig. 11e). Aside from the Gorm-Lola Ridge reverse fault, no structures directly indicate shortening below the uppermost syn-rift deposits. This implies that thick mobile evaporites can mask the effects of shortening in mildly inverted rift basins if cover structures recording shortening are unidentifiable, regional marker horizons are absent and the salt budget not constrained.

Other inverted basins in the North Sea show a similar strong control imposed by the Zechstein salt, e.g. the Broad Fourteens Basin (offshore Netherlands; e.g. Nalpas et al., 1995) and the the Sole Pit Basin (offshore UK; Glennie and Boegner, 1981; van Hoorn, 1987). Where present in these basins, its ability to decouple deformation in basement and cover strongly controlled inversion to produce structural styles comparable to those documented in our study area.

5.2 Kinematics of basement shortening

As explained above, we infer from the Late Cretaceous-Danian inversion structures that the Gorm-Tyra Fault and the Coffee Soil Fault experienced reverse slip during inversion (Fig. 12). As also mentioned, all basement faults have conserved a net normal offset in spite of basement shortening, and there are no indications of reverse slip on any of the smaller basement faults. Reactivation in the basement during inversion was therefore restricted to only the largest basement faults, which agrees with

https://doi.org/10.5194/se-2020-127
Preprint. Discussion started: 27 August 2020
© Author(s) 2020. CC BY 4.0 License.


other studies of inverted basins (e.g. Dorobek and Grimaldi, 2011; Reilly et al., 2017). As indicated by the continuous inversion margins, The Gorm-Tyra Fault and segments 2 and 3 of the Coffee Soil Fault probably reactivated along their full lengths within the visible area (see below; cf. Reilly et al., 2017). Following the eastern inversion margin, The Adda- and Igor-Emma Ridges indicate higher degrees of shortening relative to the area above the Poul Plateau, due to their large fold amplitudes. Below these ridges, the throw of the Coffee Soil Fault is significantly larger than along the Poul Plateau area as indicated by the depth to the Top Pre-Zechstein surface in the immediate hangingwall (Fig. 9a). This agrees with earlier studies in which the reverse-displacement profile along the upper parts of mildly inverted normal faults mimic that of their deeper normal-displacement profiles (Jackson et al., 2013, Reilly et al., 2017).

The triangle-zone concept of Stewart (2014) as mentioned above, offers an explanation as to why no reverse slip is evident from the upper parts of segment 1 of the Coffee Soil Fault and the Gorm-Tyra Fault (Fig. 13a). This similarity suggests a closer relationship between these faults, than between segments 1 and 2 of the Coffee Soil Fault (Fig. 12), at least during inversion. Roberts et al. (1990) provided a similar explanation of the inversion structure, Lindesnes Ridge, in the Norwegian part of the Feda Graben (Study area figure). Here, the application of the triangle-zone concept provided a simpler geometry free of inferred enigmatic basin floor dip angles or basement faults that coincidentally inverted to net zero offsets, making them invisible. In our case, the concept likewise resolves the need to include large reactivated basement faults in continuation of cover faults, where they are unlikely to exist and not indicated by the seismic data, e.g. below the Arne-Elin Graben (Fig. 4; cf. Vejbæk and Andersen, 1987; Cartwright, 1989).

Still, the possible absence of Zechstein units as indicated on Fig. 9c and the unlikelihood of a basal detachment, prove a problem for this model in parts of the Tail End Graben. This area underlies the confluence of the Arne- and Bo-Jens Ridges that both override salt ridges to the northwest and south, respectively. We speculate that folding of the cover units at their confluence account for the thin-skinned shortening above this gap in basal Zechstein units. In addition, one of the mentioned basement anticlines, which may have formed by shortening during inversion, is found in this area. This would to some degree help balance the shortening of basement and cover.

5.3 Magnitude and direction of shortening

Vejbæk and Andersen (1987; 2002) proposed that a NNE-SSW-directed shortening with a mild dextral transpressional component along NNW-SSE-striking lineaments, explains the Late Cretaceous-Danian inversion of the Danish Central Graben. They note however (2002), that N-S-striking folds (e.g. Bo-Jens Ridge and Gorm-Lola Ridge) are not consistent with this regime, and suggest that Zechstein-salt movements played a role in their formation, which we have confirmed. Cartwright (1989) discarded the need for a strike-slip component, and argued for simple NE-SW-directed shortening to explain the range of strike orientations seen in inversion folds (WNW-ESE to N-S, Fig. 11f). We tend to agree with this, as we have found few indications of strike-slip components related to inversion. The most notable of such, are the small normal faults atop the crest of the Bo-Jens Ridge (Figs. 11b and 11d). These strike c. NE-SW which is compatible with a dextral shear along the N-S-striking axis of the fold according to the oblique-inversion models of Letouzey et al. (1995).

https://doi.org/10.5194/se-2020-127
Preprint. Discussion started: 27 August 2020
© Author(s) 2020. CC BY 4.0 License.


The average NW-SE strike of the inversion-related structures indicate an apparent overall NE-SW shortening. As casually pointed out by Cartwright (1989), the total apparent shortening of the rift during Late Cretaceous-Danian inversion amounted to only "a few percent" along this axis. We have performed no quantitative analyses to test this claim as e.g. Jackson et al. (2013) did on data from the Egersund Basin. We concur though by referring to our observation that inversion-related folds are open, and that the degree of inversion (sensu Cooper et al., 1989) is low, as evident from the interpreted seismic sections and the net extensional offset on basement structures. Still, standard methods as e.g. line-length balancing have been shown to grossly underestimate the amount of shortening in physical models using wet clay (Eisenstadt and Withjack, 1995). If shortening occurred without producing significant reverse movement on basement faults, the amount of shortening due to inversion of e.g. the DCG may be higher than expected.

5.4 Mechanisms responsible for ductile deformation styles

Here, "ductile" refers to deformation that is apparently continuous at seismic scale, but may be brittle at a smaller scale. In especially the narrow northern inverted area (Figs. 5 and 11f), a significant amount of cover folding occurred during Late Cretaceous inversion, even though Zechstein salt may not have been present at depth to form a thrust detachment for this thin-skinned deformation. An overall impression of a slightly pure-shear style of shortening is apparent from the cover units in this zone, especially when also considering the gentle basin-wide flexure associated with the Paleogene Tyra-Igor Ridge. Cartwright (1989) speculated that the Late Jurassic shales in the DCG (see e.g. Michelsen et al., 2003) could have retained anomalously high pore pressures at the time of inversion and that tectonic compaction of these units could have taken up a significant amount of shortening during inversion. We concur, as this explains the high degree of folding and ductile thickening of the cover units in the mentioned area while reverse faults are less abundant. This implies that the degree of shortening could be greater than anticipated from quantitative analyses, as explained above.

Additionally, flexural slip (Tanner, 1989) probably occurred to a high degree across the inverted zones in the study area to allow the significant folding of kilometre-thick units along with often limited faulting as resolved on the seismic data, e.g. in the Bo-Jens Ridge (Fig. 6). Again, overpressure could have greatly contributed to the implied shearing parallel to bedding. This mechanism may further explain the often high degree of folding relative to faulting in the Triassic-Lower Jurassic carapace in the southern part of the study area (e.g. Fig. 7), which resulted from both tectonic extension and contraction.

6 Conclusions

Based on the mapping of surfaces and structures from a 3D seismic dataset, we have performed an analysis of structures and kinematics related to Late Cretaceous basin inversion in the Danish Central Graben. Our key conclusions are:

1. In addition to the spatial correlation of inversion zones and Late Jurassic-Early Cretaceous depocentres, the western margin of the inverted basins correlates strongly to the westwards pinch-out of Zechstein evaporites in the study area. The prominent thin-skinned inversion structures found here directly overlie and extend parallel to salt ridges and –

https://doi.org/10.5194/se-2020-127
Preprint. Discussion started: 27 August 2020
© Author(s) 2020. CC BY 4.0 License.


rollers. These populate the shallowest parts of the halfgraben slopes dipping east towards the large basement faults, Coffee Soil Fault segment 1 and the Gorm-Tyra Fault. Deformation was localized above and along the salt structures due to the reduced thickness and pre-existing faults in the cover above. The observed structural styles compare well to those produced with physical-model experiments that simulate inversion of basins with a basal layer of mobile salt, and also to structural styles found in other inverted basins with basal Zechstein evaporites in the region.

2. The eastern margin of the inverted basins follow the upper tip of the rift-bounding Coffee Soil Fault. We infer reverse reactivation of its fault segments 2 and 3 from the buttress folds in the cover units in the immediately adjacent hangingwall and the high degree of coupled deformation above and below the Zechstein units, i.e. thick-skinned inversion.
3. In the southern part of the study area where mobile Zechstein salt is abundant and widespread, the outer limits of the inverted basins sit far apart. Reverse faults soling out into a thin Triassic evaporite unit reveal thin-skinned shortening here. We infer that shortening of laterally extensive mobile-salt structures occurred as well, in spite of the lack of direct evidence hereof.
4. No basement structures unequivocally indicate post-rift shortening in our study area. To explain thin-skinned shortening in the cover units, we balance it to basement shortening qualitatively via a triangle-zone concept explained by Stewart (2014). Due to enhanced friction inhibiting slip along their upper fault planes, sub-salt reverse slip on the halfgraben-bounding basement faults led to backthrusting along a detachment in the basal Zechstein units on the halfgraben dip-slope. This effectively formed a triangle zone in the hangingwall block between the basal detachment and the subsalt fault plan. The observed thin-skinned faulting and folding high on the dip-slope are the consequence of these kinematics. Thereby, in the case of our study area, we infer reverse reactivation of the Gorm-Tyra Fault and segment 1 of the Coffee Soil Fault during basin inversion.
5. Salt migration away from some areas may have enhanced synclinal folding of the cover above during inversion. Our interpretations imply that mobile Zechstein salt was initially present in significant amounts beyond the modern-day mobile-salt pinch-out in the area. The continued migration of mobile Zechstein salt towards the northern and southern mobile-salt domains persisted into at least the Late Cretaceous.
6. We have found very few indications of strike-slip components related to inversion in the study area. We therefore conclude that c. NE-SW-directed shortening caused the basin inversion, i.e. shortening orthogonal to the overall strike trend of inversion structures. The overall degree of inversion is mild, implying a low magnitude of overall shortening. Ductile deformation of the cover units at the seismic scale accounts for some thin-skinned shortening in the study area, even in deeper parts of the cover.
7. In summary, Zechstein evaporites exerted strong controls on the development of thin-skinned faults and folds during basin inversion in the Danish Central Graben in a manner similar to those seen in other natural and experimental examples. Additionally, we infer that only the two largest sub-salt faults in our study area experienced significant reverse reactivation during inversion, i.e. the rift-bounding Coffee Soil Fault and the Gorm-Tyra fault. Our results

https://doi.org/10.5194/se-2020-127
Preprint. Discussion started: 27 August 2020
© Author(s) 2020. CC BY 4.0 License.


demonstrate that even thin evaporite units and apparent welds may be activated as detachments during inversion if their orientations are favourable, e.g. along halfgraben dip-slopes. If in addition, mobile evaporites are present in sufficient amounts to form ridges or reactive diapirs, thin-skinned folds and faults in the overburden will initiate from these, during both extension and contraction. Thick and extensive mobile evaporites may mask the effects of basin inversion in mildly inverted rift basins if cover structures recording shortening cannot be identified, or where a regional marker horizon is absent and the salt budget not constrained.

Data availability: The Danish Underground Consortium (DUC; Total E&P Denmark, Noreco and Nordsøfonden) owns the seismic data and well data used in this study. Access was granted the authors via the Danish Hydrocarbon Research and Technology Centre (DHRTC).

Author contributions: THH is the primary author of this paper and carried out the seismic interpretations and structural analyses in this study. Section 2 was written mainly by ORC. ORC and KJA provided discussions and input throughout the study, and contributed to the writing and editing of the manuscript.

Competing interests: The authors declare that they have no conflict of interest. The intellectual property rights belong to the authors and Aarhus University. DUC and DHRTC have not had any influence on the results presented in this paper.

Acknowledgements: We kindly acknowledge DUC for providing seismic and well data and for the permission to publish this work. We thank DHRTC for funding the PhD of Torsten Hundebøl Hansen, during which this study was carried out. Aarhus University and DHRTC are thanked for their support of PhD supervisors, Ole Rønø Clausen and Katrine Juul Andresen. Schlumberger and Eliis have generously provided academic licenses for the interpretation software, Petrel and Paleoscan respectively.

Financial support: This work was funded by the Danish Hydrocarbon Research and Technology Centre (DHRTC) under the Tight Reservoir Development (TRD1) programme.

References

Anell, I., Thybo, H., and Rasmussen, E.: A synthesis of Cenozoic sedimentation in the North Sea, Basin Research, 24, 154-179, 2012.

Back, S., Van Gent, H., Reuning, L., Grötsch, J., Niederau, J., and Kukla, P.: 3D seismic geomorphology and sedimentology of the Chalk Group, southern Danish North Sea, Journal of the Geological Society, 168, 393-406, 2011.

https://doi.org/10.5194/se-2020-127
Preprint. Discussion started: 27 August 2020
© Author(s) 2020. CC BY 4.0 License.


Bertelsen, F.: Lithostratigraphy and depositional history of the Danish Triassic, Danmarks Geologiske Undersogelse, Serie B, 4, 1980.

Bertram, G., and Milton, N.: Reconstructing basin evolution from sedimentary thickness; the importance of palaeobathymetric control, with reference to the North Sea, Basin Research, 1, 247-257, 1988.

Bonini, M., Sani, F., and Antonielli, B.: Basin inversion and contractional reactivation of inherited normal faults: A review based on previous and new experimental models, Tectonophysics, 522-523, 55-88, 10.1016/j.tecto.2011.11.014, 2012.

Brun, J. P., and Nalpas, T.: Graben inversion in nature and experiments, Tectonics, 15, 677-687, 10.1029/95TC03853, 1996.

Cartwright, J.: The kinematics of inversion in the Danish Central Graben, Geological Society, London, Special Publications, 44, 153-175, 1989.

Cartwright, J.: The kinematic evolution of the Coffee Soil Fault, Geological Society, London, Special Publications, 56, 29-40, 1991.

Clausen, O. R., and Korstgard, J. A.: Tertiary Tectonic Evolution Along the Arne-Elin Trend in the Danish Central Trough, Terra Nova, 5, 233-243, 1993a.

Clausen, O. R., and Korstgard, J. A.: Faults and faulting in the Horn Graben area, Danish North Sea, First Break, 11, 127-143, 1993b.

Clausen, O. R., Nielsen, S. B., Egholm, D. L., and Goledowski, B.: Cenozoic structures in the eastern North Sea Basin - A case for salt tectonics, Tectonophysics, 514, 156-167, 2012.

Clausen, O. R., Andresen, K. J., and Rasmussen, J. A.: A Late Paleozoic sill complex and related paleo-topography in the eastern North Sea analyzed using 3D seismic data, Tectonophysics, 674, 76-88, 10.1016/j.tecto.2016.02.010, 2016.

Coward, M., Dewey, J., Hempton, M., and Holroyd, J.: Tectonic evolution, The Millennium Atlas: Petroleum Geology of the Central and Northern North Sea. Geological Society, London, 17, 33, 2003.

Damtoft, K., Andersen, C., and Thomsen, E.: Prospectivity and hydrocarbon plays of the Danish Central Trough, Petroleum geology of north west Europe. Proc. 3rd conference London, 1986. Vol. 1, 403-417, 1987.

Duffy, O. B., Gawthorpe, R. L., Docherty, M., and Brocklehurst, S. H.: Mobile evaporite controls on the structural style and evolution of rift basins: Danish Central Graben, North Sea, Basin Research, 25, 310-330, 2013.

Eisenstadt, G., and Withjack, M. O.: Estimating inversion: results from clay models, Basin inversion, 119-136, 1995.

Ferrer, O., McClay, K., and Sellier, N.: Influence of fault geometries and mechanical anisotropies on the growth and inversion of hanging-wall synclinal basins: insights from sandbox models and natural examples, Geological Society, London, Special Publications, 439, 487-509, 2017.

Glennie, K., and Boegner, P.: Sole pit inversion tectonics, Petroleum Geology of the Continental Shelf of North-West Europe. Heyden, London, 110-120, 1981.

Glennie, K. W., Higham, J., and Stemmerik, L.: Permian, in: The Millennium Atlas: Petroleum Geology of the Central and Northern North Sea, edited by: Evans, D., Armour, C. G. A., and Bathurst, P., The Geological Society of London, London, 91-103, 2003.

https://doi.org/10.5194/se-2020-127
Preprint. Discussion started: 27 August 2020
© Author(s) 2020. CC BY 4.0 License.


Goldsmith, P., Hudson, G., Van Veen, P., Evans, D., Graham, C., Armour, A., and Bathurst, P.: Triassic, The Millennium Atlas: Petroleum Geology of the Central and Northern North Sea. Geological Society, London, 105, 127, 2003.

Gołedowski, B., Nielsen, S. B., and Clausen, O. R.: Patterns of Cenozoic sediment flux from western Scandinavia, Basin Research, 24, 377-400, 2012.

Gowers, M. B., and Sæbøe, A.: On the structural evolution of the Central Trough in the Norwegian and Danish sectors of the North Sea, Marine and Petroleum Geology, 2, 298-318, 1985.

Grimaldi, G. O., and Dorobek, S. L.: Fault framework and kinematic evolution of inversion structures: Natural examples from the Neuquén Basin, Argentina, AAPG Bulletin, 95, 27-60, 10.1306/06301009165, 2011.

Jackson, M. P. A., and Talbot, C. J.: External shapes, strain rates, and dynamics of salt structures, Geological Society of America Bulletin, 97, 305-323, 10.1130/0016-7606(1986)97<305:ESSRAD>2.0.CO;2, 1986.

Jackson, C. A. L., and Larsen, E.: Temporal constraints on basin inversion provided by 3D seismic and well data: a case study from the South Viking Graben, offshore Norway, 20, 397-417, 10.1111/j.1365-2117.2008.00359.x, 2008.

Jackson, C.-L., Chua, S.-T., Bell, R., and Magee, C.: Structural style and early stage growth of inversion structures: 3D seismic insights from the Egersund Basin, offshore Norway, Journal of Structural Geology, 46, 167-185, 2013.

Jackson, C. A. L., Rodriguez, C. R., Rotevatn, A., and Bell, R. E.: Geological and geophysical expression of a primary salt weld: An example from the Santos Basin, Brazil, Interpretation, 2, SM77-SM89, 10.1190/INT-2014-0066.1, 2014.

Jagger, L. J., and McClay, K. R.: Analogue modelling of inverted domino-style basement fault systems, Basin Research, 30, 363-381, 2018.

Jakobsen, F.: Late Cretaceous stratigraphy and basin development in the Danish Central Graben, 1-49, 2014.

Jarsve, E. M., Maast, T. E., Gabrielsen, R. H., Faleide, J. I., Nystuen, J. P., and Sassier, C.: Seismic stratigraphic subdivision of the Triassic succession in the Central North Sea; integrating seismic reflection and well data, Journal of the Geological Society, 171, 353-374, 10.1144/jgs2013-056, 2014.

Kockel, F.: Inversion structures in Central Europe - Expressions and reasons, an open discussion, Geologie en Mijnbouw/Netherlands Journal of Geosciences, 82, 367-382, 2003.

Koopman, A., Speksnijder, A., and Horsfield, W. T.: Sandbox model studies of inversion tectonics, Tectonophysics, 137, 379-388, 10.1016/0040-1951(87)90329-5, 1987.

Korstgård, J. A., Lerche, I., Mogensen, T. E., and Thomsen, R. O.: Salt and fault interactions in the northeastern Danish Central Graben: observations and inferences., Bulletin of the Geological Society of Denmark, 40, 197-255, 1993.

Lassen, A., and Thybo, H.: Neoproterozoic and Palaeozoic evolution of SW Scandinavia based on integrated seismic interpretation, Precambrian Research, 204-205, 75-104, 2012.

Letouzey, J.: Fault reactivation, inversion and fold-thrust belt, Petroleum and tectonics in mobile belts, 101-128, 1990.

Letouzey, J., Werner, P., and Marty, A.: Fault reactivation and structural inversion. Backarc and intraplate compressive deformations. Example of the eastern Sunda shelf (Indonesia), Tectonophysics, 183, 341-362, https://doi.org/10.1016/0040-1951(90)90425-8, 1990.

https://doi.org/10.5194/se-2020-127
Preprint. Discussion started: 27 August 2020
© Author(s) 2020. CC BY 4.0 License.


Letouzey, J., Colletta, B., Vially, R., Chermette, J. C., Jackson, M. P. A., Roberts, D. G., and Snelson, S.: Evolution of Salt-Related Structures in Compressional Settings, in: Salt Tectonics: A Global Perspective, American Association of Petroleum Geologists, 0, 1995.

McClay, K. R.: Analogue models of inversion tectonics, Inversion tectonics, 41-59, 1989.

McClay, K. R.: The geometries and kinematics of inverted fault systems: a review of analogue model studies, Geological Society, London, Special Publications, 88, 97-118, 1995.

McKenzie, D.: Some remarks on the development of sedimentary basins, Earth and Planetary Science Letters, 40, 25-32, 10.1016/0012-821X(78)90071-7, 1978.

McKie, T., Jolley, S., and Kristensen, M.: Stratigraphic and structural compartmentalization of dryland fluvial reservoirs: Triassic Heron Cluster, Central North Sea, Geological Society, London, Special Publications, 347, 165-198, 2010.

Megson, J.: The North Sea Chalk Play: examples from the Danish Central Graben, Geological Society, London, Special Publications, 67, 247-282, 1992.

Michelsen, O., and Clausen, O. R.: Detailed stratigraphic subdivision and regional correlation of the southern Danish Triassic succession, Marine and Petroleum Geology, 19, 563-587, 2002.

Michelsen, O., Nielsen, L. H., Johannessen, P. N., Andsbjerg, J., and Surlyk, F.: Jurassic lithostratigraphy and stratigraphic development onshore and offshore Denmark, Geological Survey of Denmark and Greenland Bulletin, 1, 147-216, 2003.

Mogensen, T. E., and Korstgård, J. A.: Triassic and Jurassic transtension along part of the Sorgenfrei-Tornquist Zone in the Danish Kattegat, Geological Survey of Denmark and Greenland Bulletin 1, 439-458, 2003.

Møller, J. J., and Rasmussen, E. S.: Middle Jurassic-Early Cretaceous rifting of the Danish Central Graben, Geological Survey of Denmark and Greenland Bulletin, 1, 247-264, 2003.

Nalpas, T., and Brun, J. P.: Salt flow and diapirism related to extension at crustal scale, Tectonophysics, 228, 349-362, 10.1016/0040-1951(93)90348-N, 1993.

Nalpas, T., Le Douaran, S., Brun, J. P., Unternehr, P., and Richert, J. P.: Inversion of the Broad Fourteens Basin (offshore Netherlands), a small-scale model investigation, Sedimentary Geology, 95, 237-250, 10.1016/0037-0738(94)00113-9, 1995.

Rank-Friend, M., and Elders, C. F.: The evolution and growth of central graben salt structures, Salt Dome Province, Danish North Sea, Geological Society, London, Memoirs, 29, 149-164, 2004.

Reilly, C., Nicol, A., and Walsh, J.: Importance of pre-existing fault size for the evolution of an inverted fault system, Geological Society, London, Special Publications, 439, 447-463, 2017.

Roberts, A. M., Yielding, G., and Badley, M. E.: A kinematic model for the orthogonal opening of the late Jurassic North Sea rift system, Denmark-mid Norway, Tectonic evolution of the North Sea rifts, 180-199, 1990.

Roma, M., Ferer, O., McClay, K. R., Muñoz, J. A., Roca i Abella, E., Gratacós, O., and Cabello López, P.: Weld kinematics of syn-rift salt during basement-involved extension and subsequent inversion: Results from analog models, Geologica acta, 16, 0391-0410, 2018a.

https://doi.org/10.5194/se-2020-127
Preprint. Discussion started: 27 August 2020
© Author(s) 2020. CC BY 4.0 License.


Roma, M., Vidal-Royo, O., McClay, K., Ferrer, O., and Muñoz, J. A.: Tectonic inversion of salt-detached ramp-syncline basins as illustrated by analog modeling and kinematic restoration, Interpretation, 6, T127-T144, 2018b.

Schiøler, P., Andsbjerg, J., Clausen, O. R., Dam, G., Dybkjær, K., Hamberg, L., Heilmann-Clausen, C., Johannessen, E. P., Kristensen, L. E., and Prince, I.: Lithostratigraphy of the Palaeogene–lower Neogene succession of the Danish North Sea, GEUS Bulletin, 12, 1-77, 2007.

Sclater, J. G., and Christie, P. A. F.: Continental stretching: an explanation of the post-mid-Cretaceous subsidence of the central North Sea Basin, Journal of Geophysical Research B: Solid Earth, 85, 3711-3739, 1980.

Stemmerik, L., Ineson, J. R., and Mitchell, J. G.: Stratigraphy of the Rotliegend group in the Danish part of the Northern Permian Basin, North Sea, Journal of the Geological Society, 157, 1127-1136, 2000.

Stewart, S. A., and Clark, J. A.: Impact of salt on the structure of the Central North Sea hydrocarbon fairways, Geological Society, London, Petroleum Geology Conference series, 1999, 179-200,

Stewart, S. A.: Detachment-controlled triangle zones in extension and inversion tectonics, Interpretation-a Journal of Subsurface Characterization, 2, Sm29-Sm38, 2014.

Surlyk, F., Dons, T., Clausen, C. K., and Higham, J.: Upper cretaceous, The Millennium Atlas: Petroleum Geology of the Central and Northern North Sea. Geological Society, London, 213, 233, 2003.

Sørensen, K.: Danish Basin subsidence by Triassic rifting on a lithosphere cooling background, Nature, 319, 660-663, 1986.

Tanner, P. W. G.: The flexural-slip mechanism, Journal of Structural Geology, 11, 635-655, 1989.

Turner, J. P., and Williams, G. A.: Sedimentary basin inversion and intra-plate shortening, Earth-Science Reviews, 65, 277-304, 2004.

Van Buchem, F. S. P., Smit, F. W. H., Buijs, G. J. A., Trudgill, B., and Larsen, P.-H.: Tectonostratigraphic framework and depositional history of the Cretaceous–Danian succession of the Danish Central Graben (North Sea)–new light on a mature area, Geological Society, London, Petroleum Geology Conference series, 2018, 9-46,

Van Hoorn, B.: Structural evolution, timing and tectonic style of the Sole Pit inversion, Tectonophysics, 137, 239-284, 1987.

Vejbaek, O. V.: Seismic stratigraphy and tectonic evolution of the Lower Cretaceous in the Danish Central Trough, 11, Danmarks Geologiske Undersøgelse, 1986.

Vejbaek, O. V., and Andersen, C.: Cretaceous Early Tertiary Inversion Tectonism in the Danish Central Trough, Tectonophysics, 137, 221-&, 1987.

Vejbaek, O. V., and Andersen, C.: Post mid-Cretaceous inversion tectonics in the Danish Central Graben - regionally synchronous tectonic events?, Bulletin of the Geological Society of Denmark, 49, 129-144, 2002.

Vejbæk, O. V.: The Horn Graben, and its relationship to the Oslo Graben and the Danish Basin, Tectonophysics, 187, 29-49, 1990.

Vejbæk, O. V.: Dybe strukturer i danske sedimentære bassiner, Geologisk Tidsskrift, 4, 1-31, 1997.

Vendeville, B. C.: Champs de failles et tectonique en extension : Modélisation expérimentale. Tectonique., Université Rennes 1,, France, 1-395 pp., 1987.

https://doi.org/10.5194/se-2020-127
Preprint. Discussion started: 27 August 2020
© Author(s) 2020. CC BY 4.0 License.


Vendeville, B. C., and Jackson, M. P. A.: The rise of diapirs during thin-skinned extension, Marine and Petroleum Geology, 9, 331-354, 1992a.

Vendeville, B. C., and Jackson, M. P. A.: The fall of diapirs during thin-skinned extension, Marine and Petroleum Geology, 9, 354-371, 1992b.

Williams, G., Powell, C., and Cooper, M.: Geometry and kinematics of inversion tectonics, Geological Society, London, Special Publications, 44, 3-15, 1989.

Withjack, M. O., and Callaway, S.: Active normal faulting beneath a salt layer: an experimental study of deformation patterns in the cover sequence, AAPG bulletin, 84, 627-651, 2000.

Yamada, Y., and McClay, K.: 3-D analog modeling of inversion thrust structures, 2004.

Ziegler, P.: Geological Atlas of Western and Central Europe, Shell Internationale Petroleum Maatschappij B.V., the Hague, 238 pp., 1990.

https://doi.org/10.5194/se-2020-127
Preprint. Discussion started: 27 August 2020
© Author(s) 2020. CC BY 4.0 License.

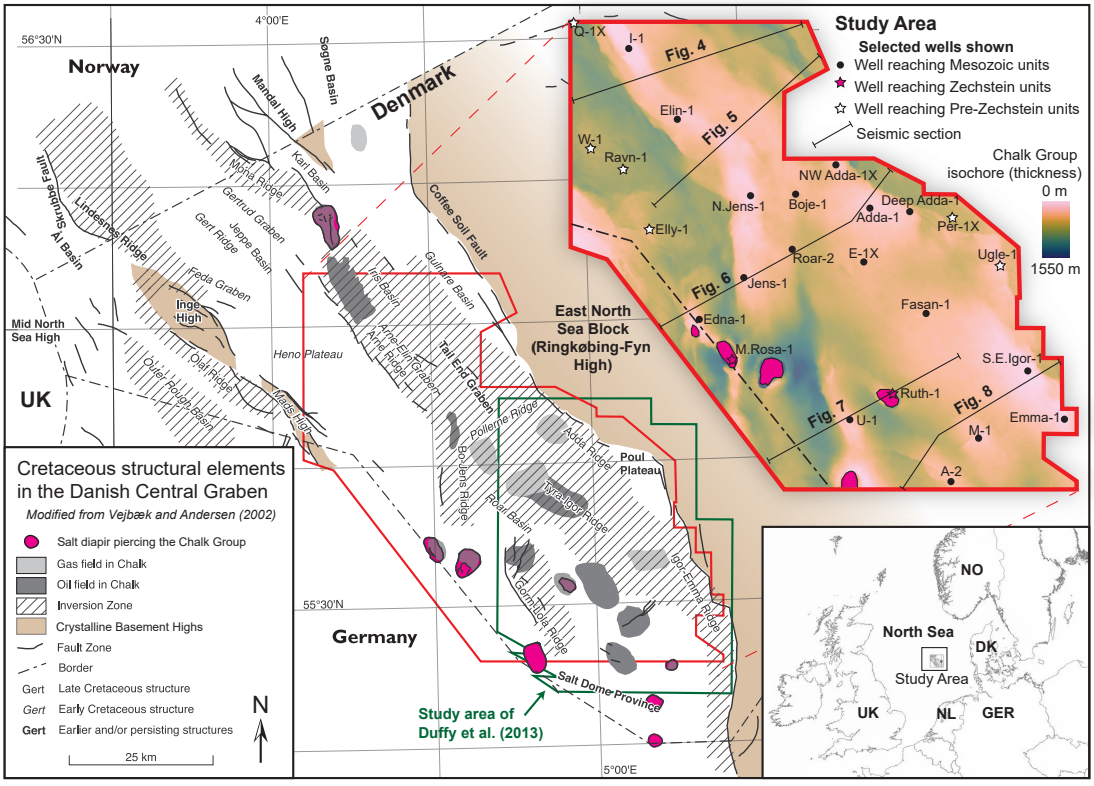

Figure 1: The Danish Central Graben with Cretaceous structural elements and inverted areas indicated. The oil and gas fields are not exhaustive for the area. The position of the area in the North Sea region is illustrated in the lower right. An enlarged map of our study area shows selected wells used in the study and interpreted seismic sections; colours indicate the Chalk Group thickness. The colour scale used (Batlow) was constructed by Crameri (2018).

https://doi.org/10.5194/se-2020-127
Preprint. Discussion started: 27 August 2020
© Author(s) 2020. CC BY 4.0 License.

Solid Earth
Discussions
Open Access
EGU

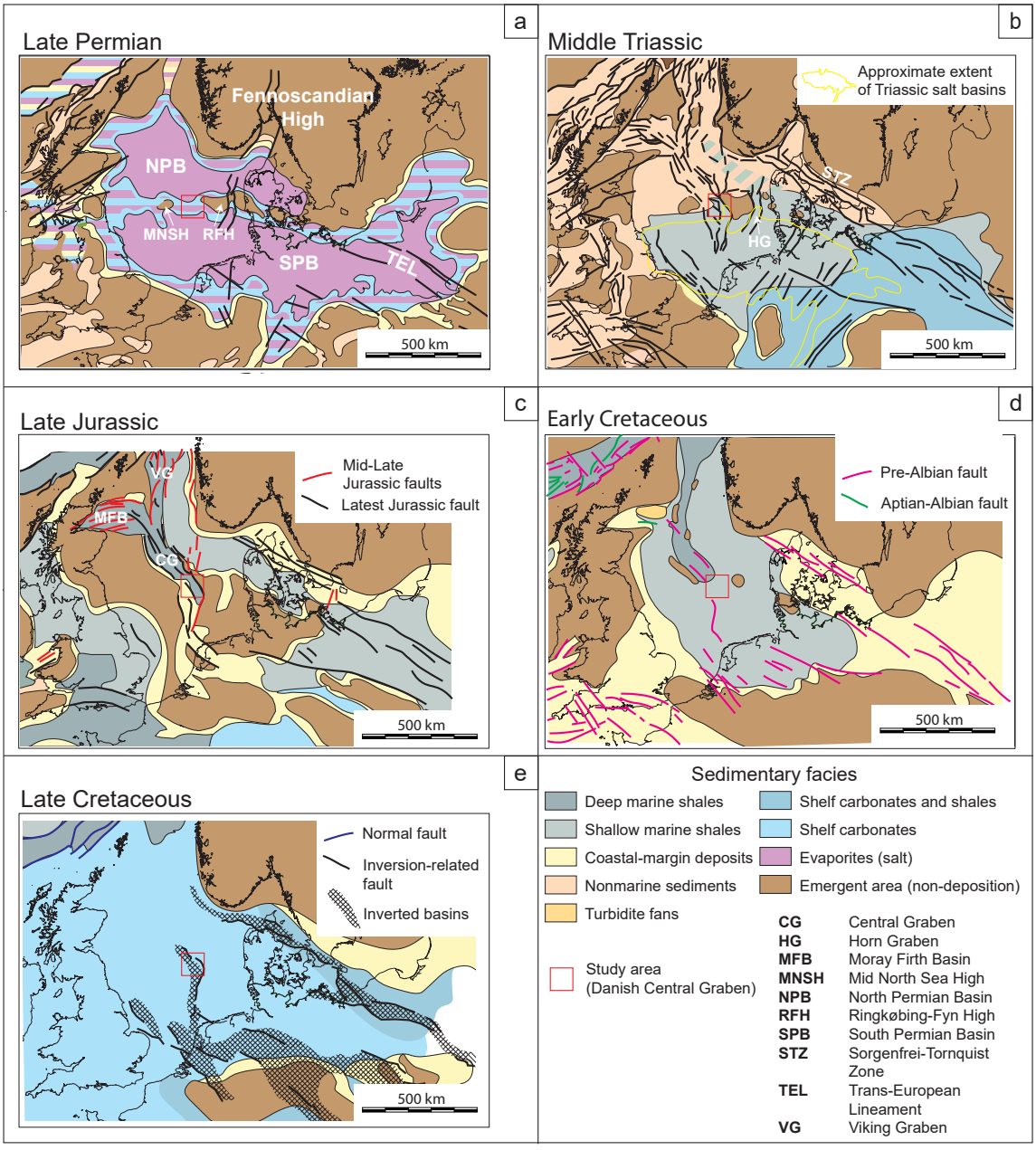

Figure 2: Palinspastic maps of the North Sea region indicating the distribution of active large-scale structures and general sedimentary facies at different periods (modified from Ziegler, 1990 and Coward et al., 2003). Modern-day coastlines are shown for reference. (a) Late Permian; (b) Middle Triassic; (c) Late Jurassic; (d) Early Cretaceous; (e) Late Cretaceous. Indicated inverted areas are from Kley (2018).

https://doi.org/10.5194/se-2020-127
Preprint. Discussion started: 27 August 2020
© Author(s) 2020. CC BY 4.0 License.

Solid Earth
Discussions
Open Access
EGU

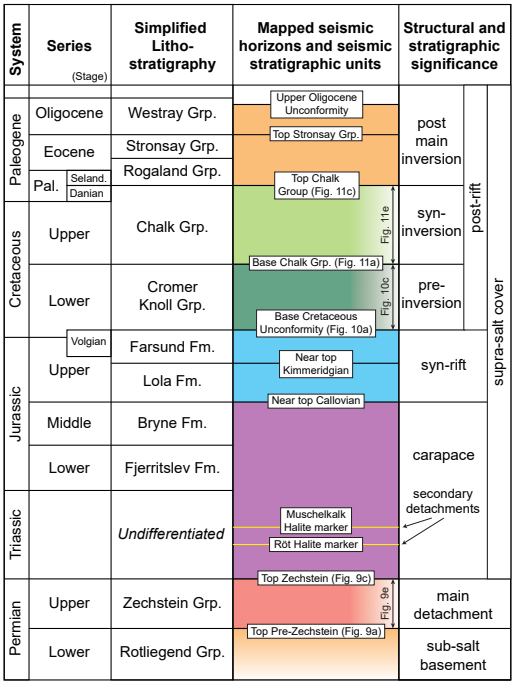

Figure 3: Stratigraphic table indicating the seismic surfaces and stratigraphic units used for this study. Other figures presenting depth and isochore maps are referenced. In the rightmost column, the structural and stratigraphic significance of each unit is indicated. Simplified Jurassic lithostratigraphic units are from Michelsen et al. (2003) and Paleogene units are from Schiøler et al. (2007).

https://doi.org/10.5194/se-2020-127
Preprint. Discussion started: 27 August 2020
© Author(s) 2020. CC BY 4.0 License.

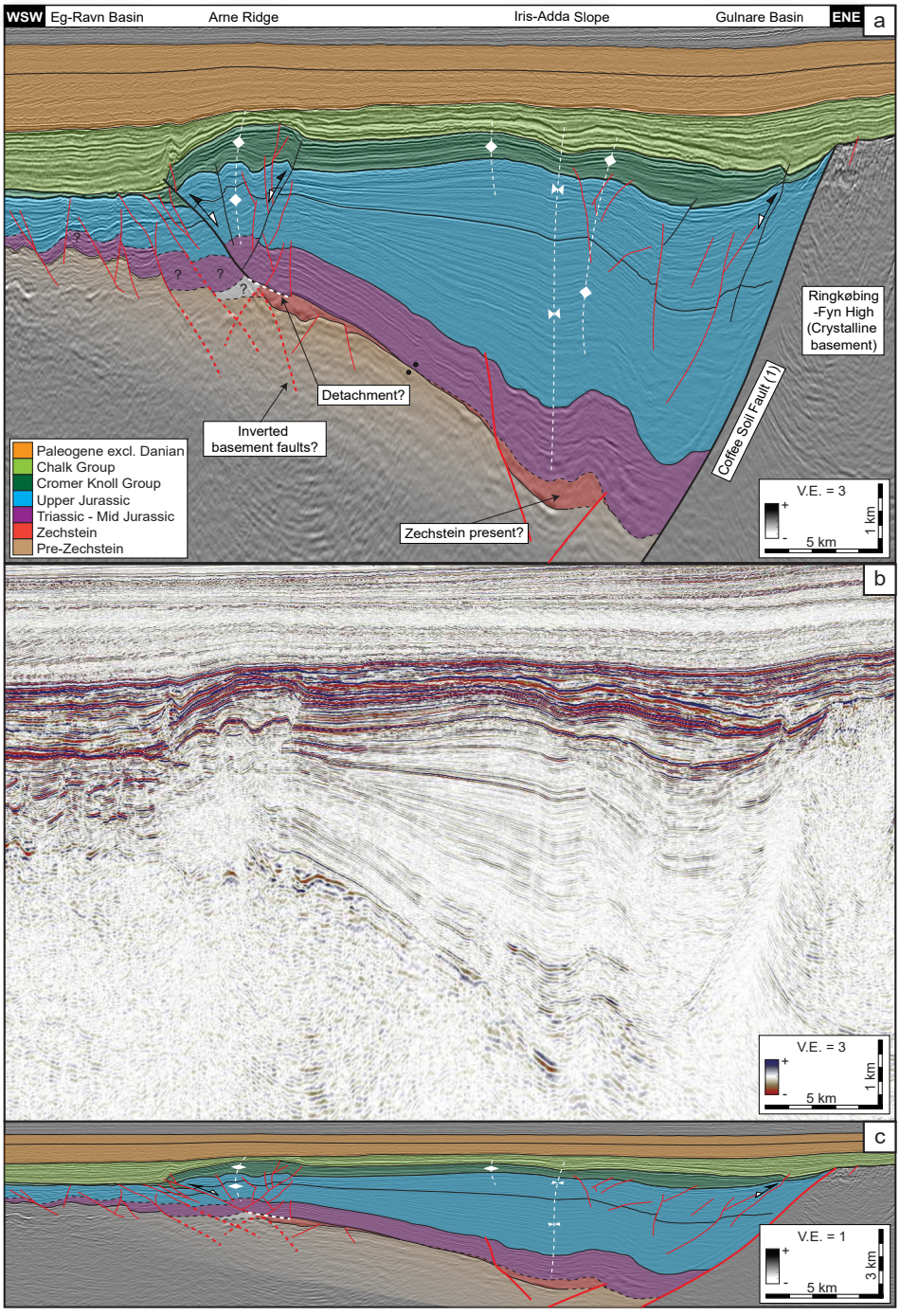

Figure 4: (a) Interpreted seismic section across the Arne Ridge and Coffee Soil Fault (segment 1). The Tyra-Igor Ridge (Paleogene inversion) is indicated also. The prominent Arne Ridge formed with the inversion of the Arne-Elin Graben above the western limit of the Zechstein units. Note the lack of buttressed folds in the immediate hangingwall of the Coffee Soil Fault. Named structures in the header and marked fold axes indicate Late Cretaceous-Danian topographical elements unless otherwise noted. (b) Uninterpreted section. (c) Interpreted section with no vertical exaggeration. An overview of the stratigraphic units and mapped surfaces is found in Fig. 3. The location of the section is indicated in Figs. 1, 9c, 10a and 11c. Seismic data supplied by DUC.

https://doi.org/10.5194/se-2020-127
Preprint. Discussion started: 27 August 2020
© Author(s) 2020. CC BY 4.0 License.

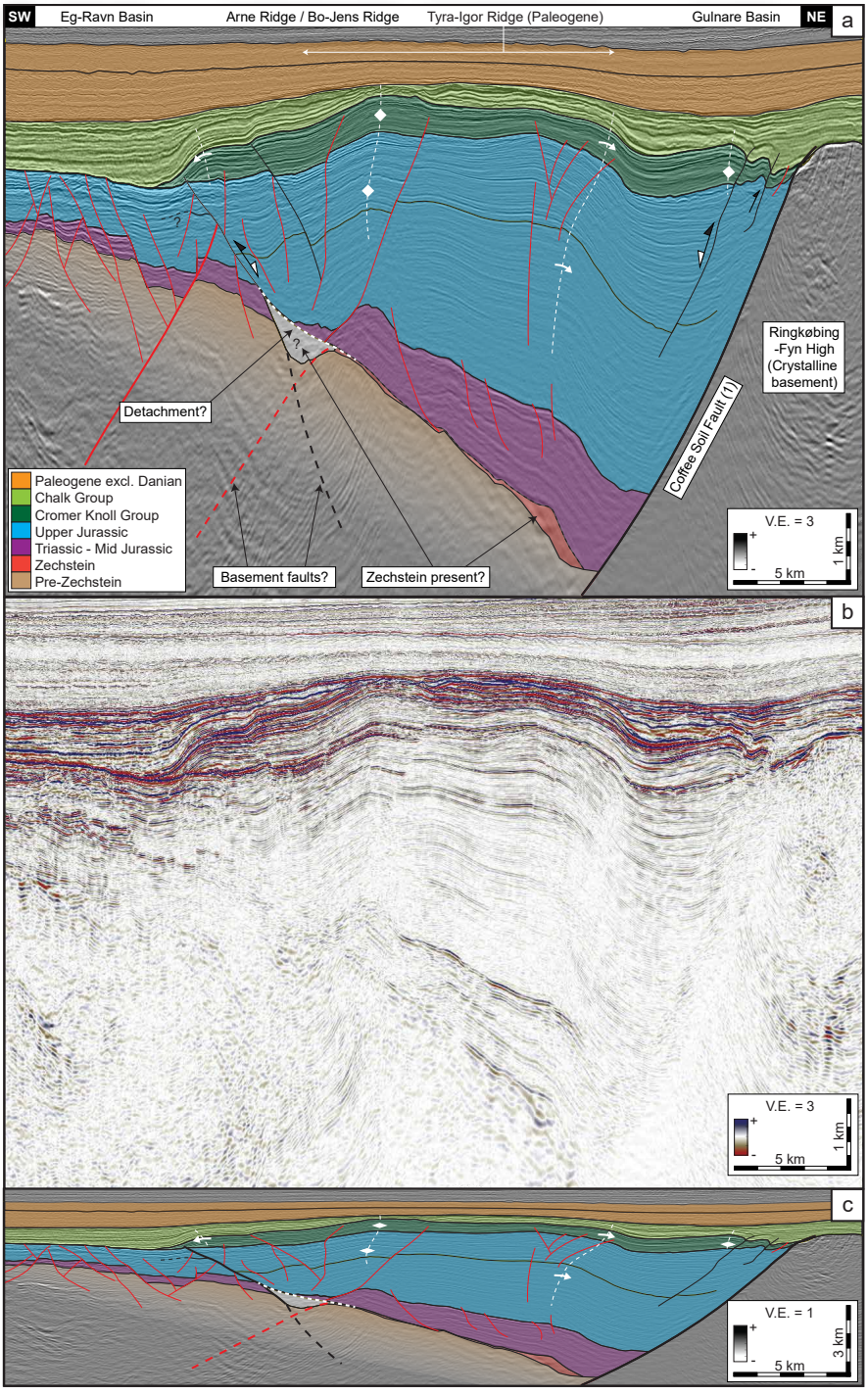

Figure 5: (a) Interpreted seismic section across the confluence of the Arne- and Bo-Jens Ridges, and Coffee Soil Fault (segment 1). Zechstein units may be absent in this area, although they are indicated. Note the high degree of folding in the sedimentary cover relative to reverse throw on inverted faults. Named structures in the header and marked fold axes indicate Late Cretaceous-Danian topographical elements unless otherwise noted. (b) Uninterpreted section. (c) Interpreted section with no vertical exaggeration. An overview of the stratigraphic units and mapped surfaces is found in Fig. 3. The location of the section is indicated in Figs. 1, 9c, 10a and 11c. Seismic data supplied by DUC.

https://doi.org/10.5194/se-2020-127
Preprint. Discussion started: 27 August 2020
© Author(s) 2020. CC BY 4.0 License.

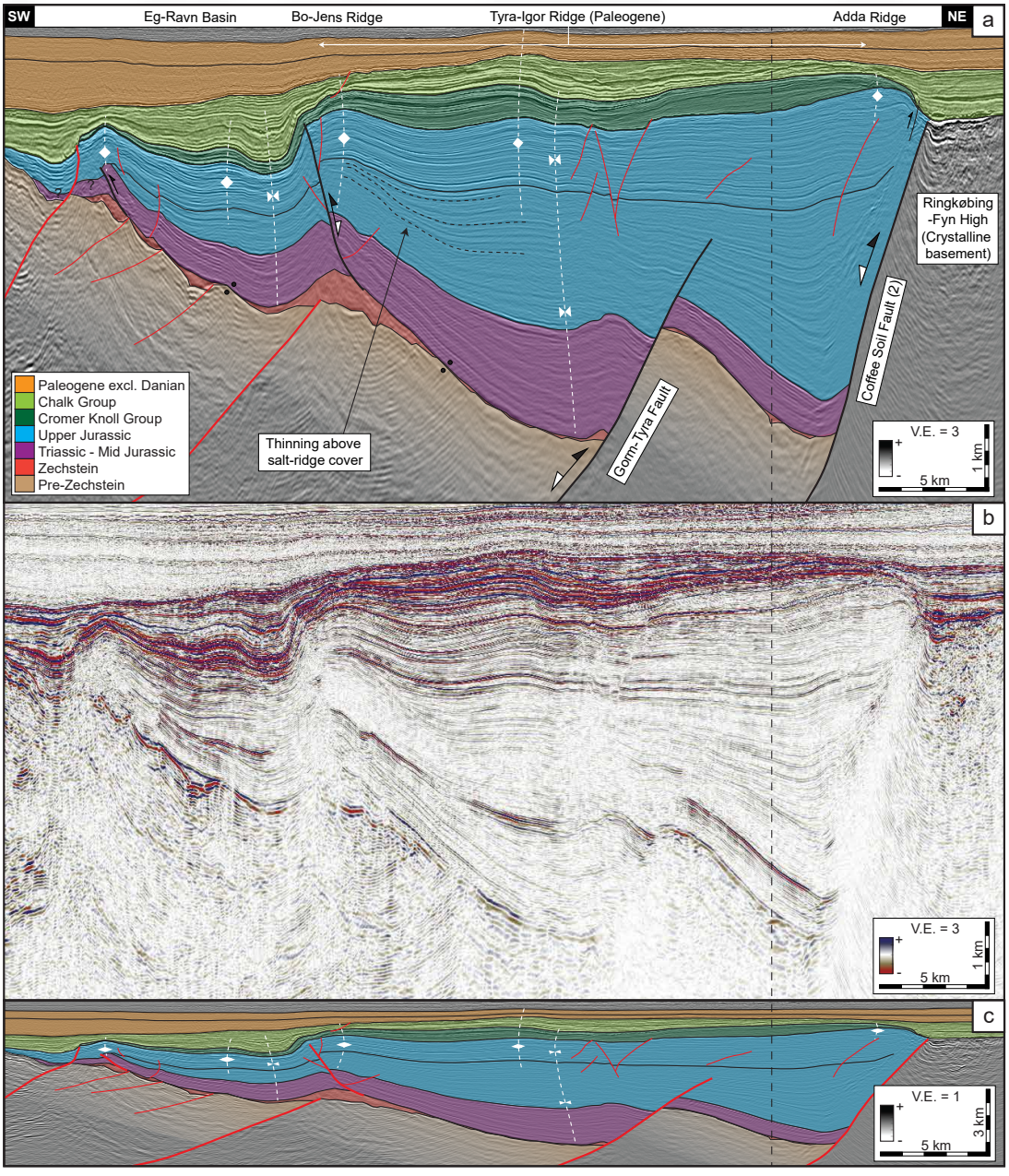

Figure 6: (a) Interpreted seismic section across the Bo-Jens- and Adda Ridges. The Tyra-Igor Ridge (Paleogene inversion) is indicated also. Note the thin-skinned structures detached by Zechstein units and a salt roller in the left portion of the section. Indicated synclines can be traced deep into the cover units. Named structures in the header and marked fold axes indicate Late Cretaceous-Danian topographical elements unless otherwise noted. (b) Uninterpreted section. (c) Interpreted section with no vertical exaggeration. An overview of the stratigraphic units and mapped surfaces is found in Fig. 3. The location of the section is indicated in Figs. 1, 9c, 10a and 11c. Seismic data supplied by DUC.

https://doi.org/10.5194/se-2020-127
Preprint. Discussion started: 27 August 2020
© Author(s) 2020. CC BY 4.0 License.

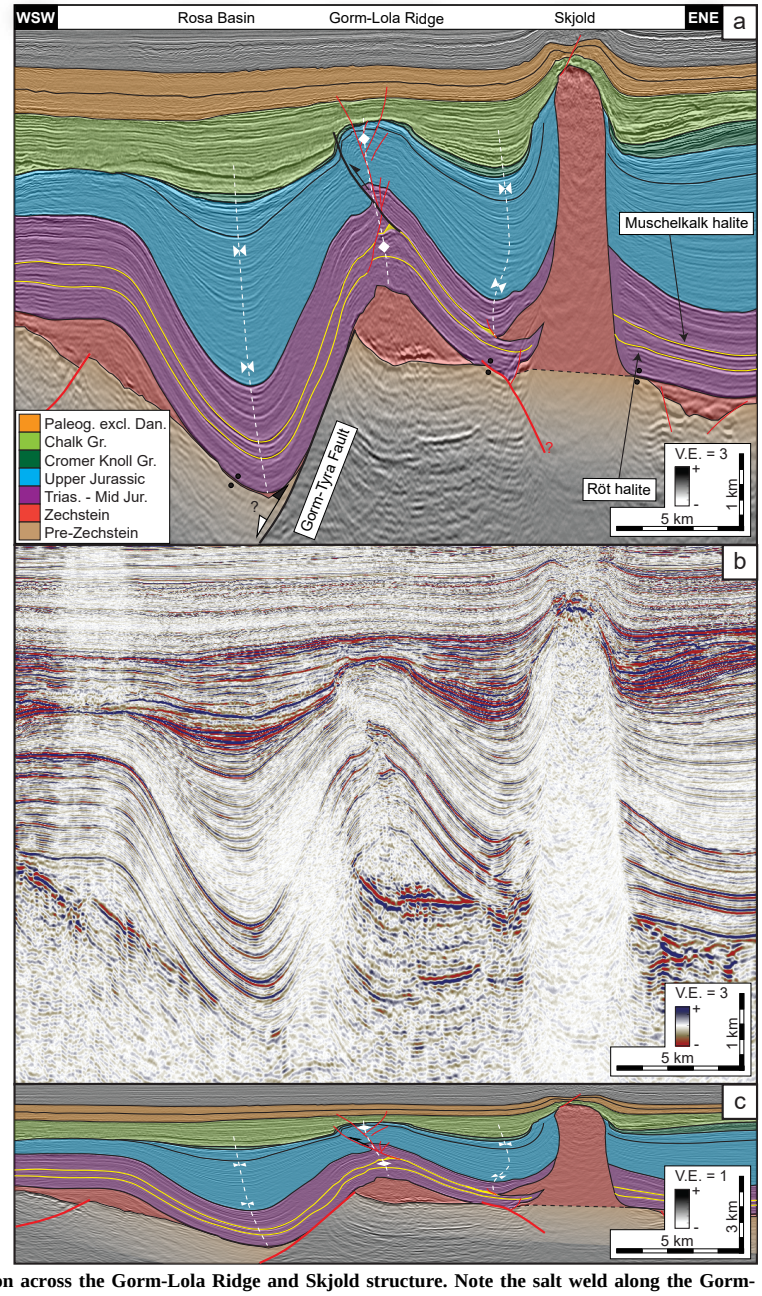

Figure 7: (a) Interpreted seismic section across the Gorm-Lola Ridge and Skjold structure. Note the salt weld along the Gorm-Tyra fault surface and the position of the Gorm-Lola ridge above the Lola Salt structure. A thin-skinned reverse fault sole out into a detachment along a Triassic evaporite layer in the flank of the structure. Named structures in the header and marked fold axes indicate Late Cretaceous-Danian topographical elements unless otherwise noted. (b) Uninterpreted section. (c) Interpreted section with no vertical exaggeration. An overview of the stratigraphic units and mapped surfaces is found in Fig. 3. The location of the section is indicated in Figs. 1, 9c, 10a and 11c. Seismic data supplied by DUC.

https://doi.org/10.5194/se-2020-127
Preprint. Discussion started: 27 August 2020
© Author(s) 2020. CC BY 4.0 License.

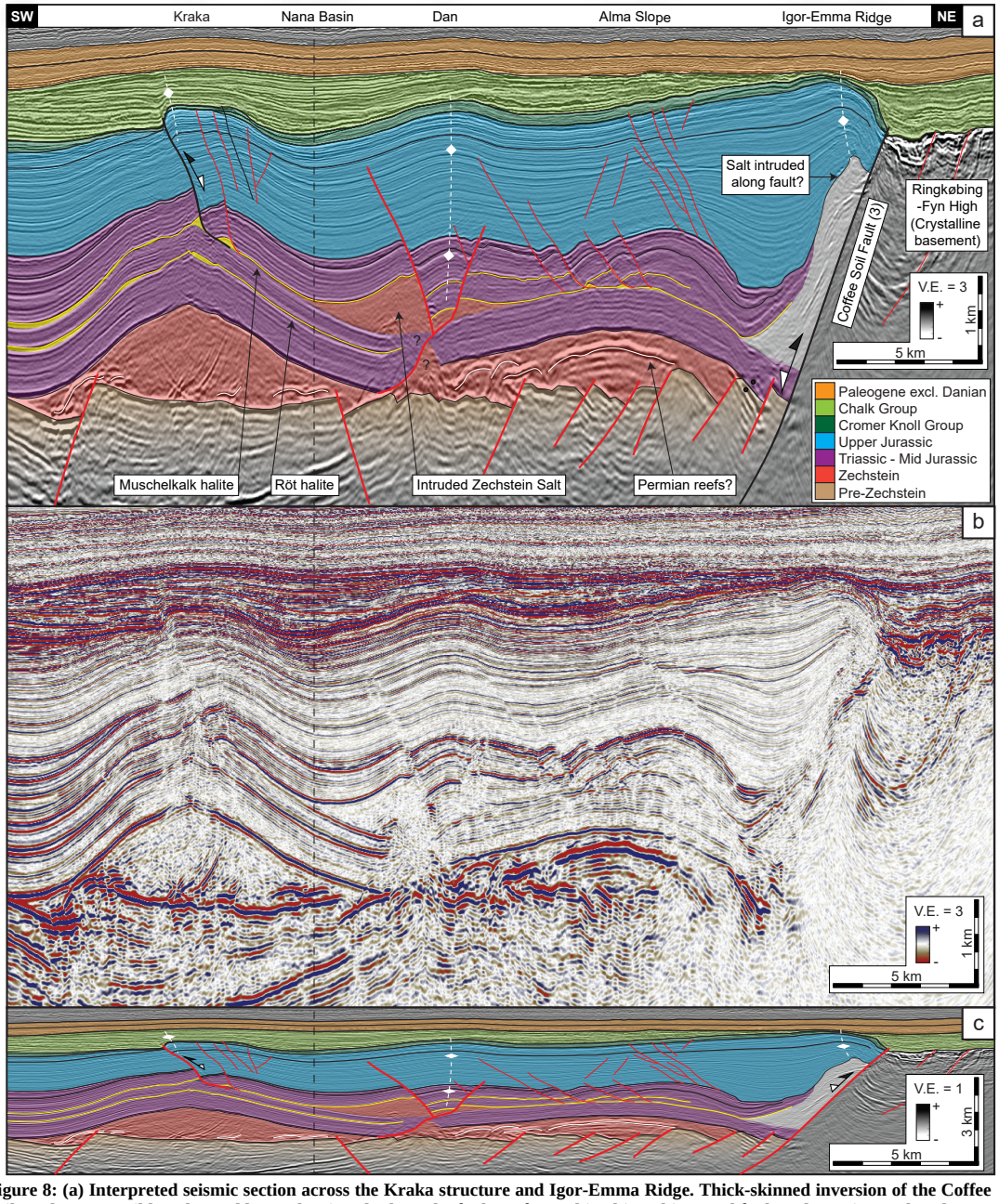

Figure 8: (a) Interpreted seismic section across the Kraka structure and Igor-Emma Ridge. Thick-skinned inversion of the Coffee Soil Fault was possibly enhanced by Zechstein salt along the fault surface. Thin-skinned inverted faults sole out into a detachment in the Muschelkalk halite on the NE flank of the Kraka pillow carapace. In the Dan structure, Zechstein salt has intruded along the Triassic evaporite layers. Late Cretaceous folding above it is evident. Named structures in the header and marked fold axes indicate Late Cretaceous-Danian topographical elements unless otherwise noted. (b) Uninterpreted section. (c) Interpreted section with no vertical exaggeration. An overview of the stratigraphic units and mapped surfaces is found in Fig. 3. The location of the section is indicated in Figs. 1, 9c, 10a and 11c. Seismic data supplied by DUC.

https://doi.org/10.5194/se-2020-127
Preprint. Discussion started: 27 August 2020
© Author(s) 2020. CC BY 4.0 License.

Solid Earth
Discussions
Open Access
EGU

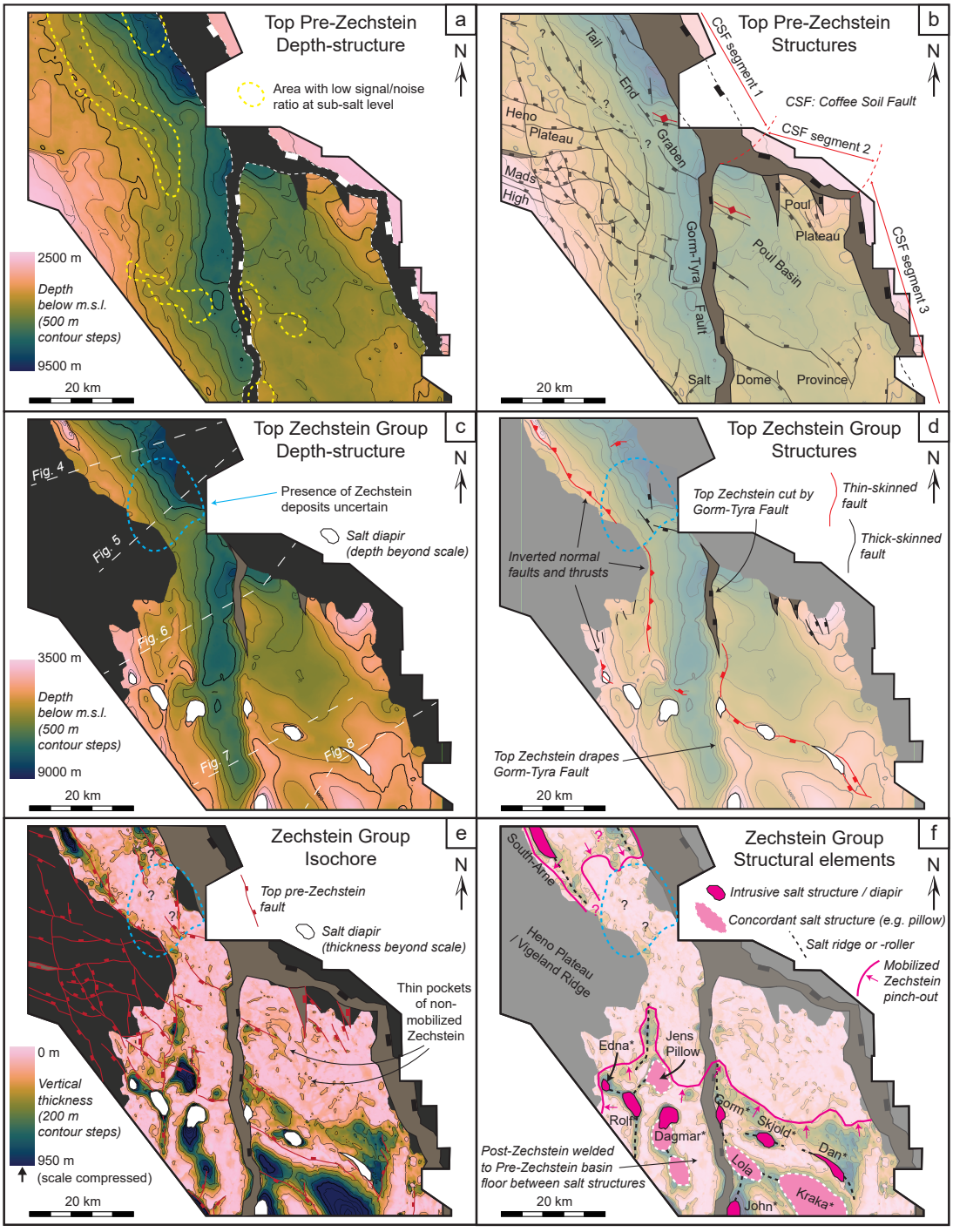

https://doi.org/10.5194/se-2020-127
Preprint. Discussion started: 27 August 2020
© Author(s) 2020. CC BY 4.0 License.

Figure 9: Depth- and structure maps constructed from seismic data illustrating the deformational geometries and extent of the sub-salt basement and the Zechstein (salt) units. (a) Top-Pre Zechstein depth and (b) -structures; (c) Top Zechstein Group depth and (d) –structures. Note the distinction between thick-skinned faults that are linked between the cover and basement, and thin-skinned faults that sole out into Zechstein units. Within the area outlined in bright blue, no wells penetrate to Zechstein levels, and the conspicuous contrast between the smooth Top-Zechstein reflection and the rugged Top Pre-Zechstein reflection is not present as in other areas (compare Fig. 5 and e.g. Fig. 7). If Zechstein units are present here, it may be only as a thin succession of marginal facies. (e) Zechstein Group isochore (thickness) map and (f) -structural elements. Major mobile-salt structures are indicated as well as the current-day pinch-out of mobilized Zechstein salt. An overview of the stratigraphic units and mapped surfaces is found in Fig. 3. The colour scale used (Batlow) was constructed by Crameri (2018).

https://doi.org/10.5194/se-2020-127
Preprint. Discussion started: 27 August 2020
© Author(s) 2020. CC BY 4.0 License.

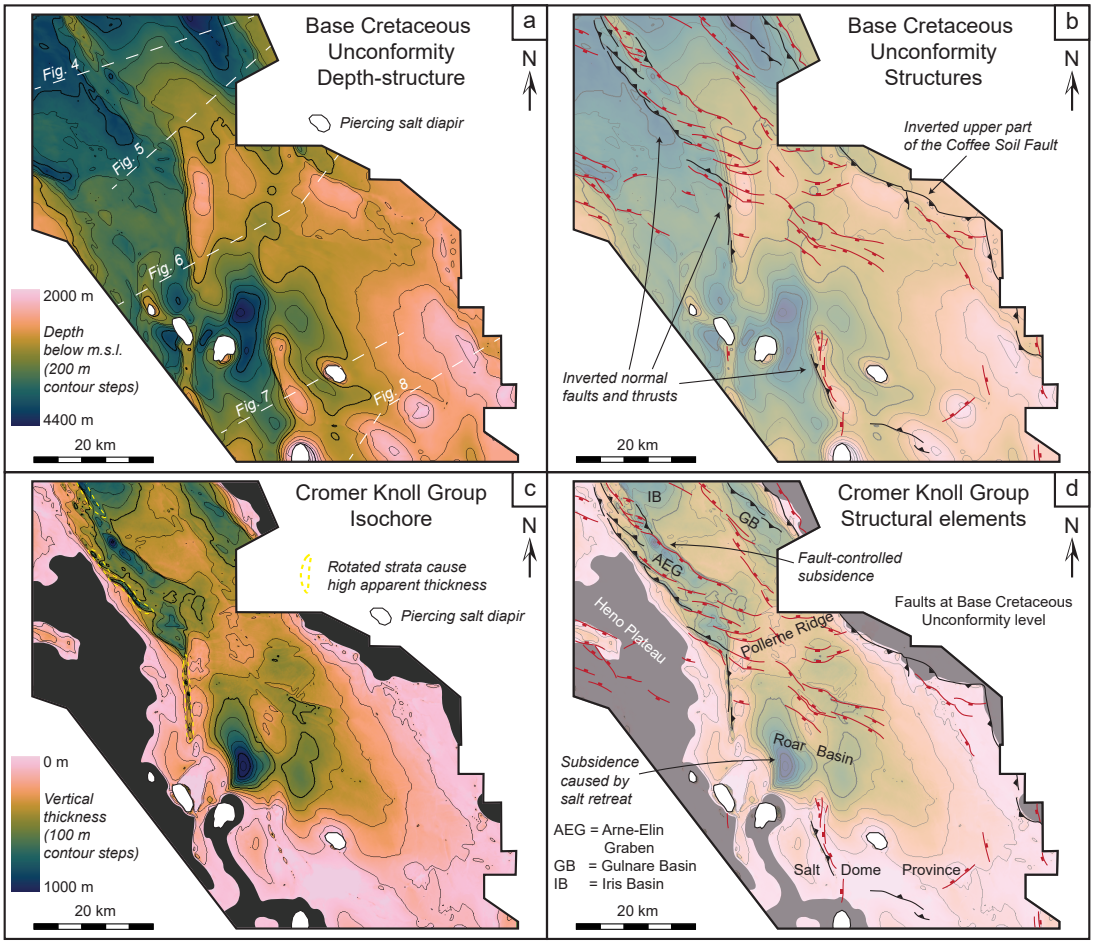

Figure 10: Depth- and structure maps constructed from seismic data illustrating the deformational geometries and extent of the Cromer Knoll Group (Lower Cretaceous, post-rift and pre-inversion). (a) Base Cretaceous Unconformity depth and (b) -structures. The fault map illustrates the selective inversion of inherited normal faults during Late Cretaceous shortening, which caused the abundance of reverse faults and thrusts at this level. (c) Cromer Knoll Group isochore (thickness) map and (d) -structural elements. These illustrate the pre-inversion position of depocentres in the study area. Thickness changes can be linked to migration of mobile Zechstein salt towards the northwest and south respectively. An overview of the stratigraphic units and mapped surfaces is found in Fig. 3. The colour scale used (Batlow) was constructed by Crameri (2018).

https://doi.org/10.5194/se-2020-127
Preprint. Discussion started: 27 August 2020
© Author(s) 2020. CC BY 4.0 License.

Solid Earth
Discussions
Open Access
EGU

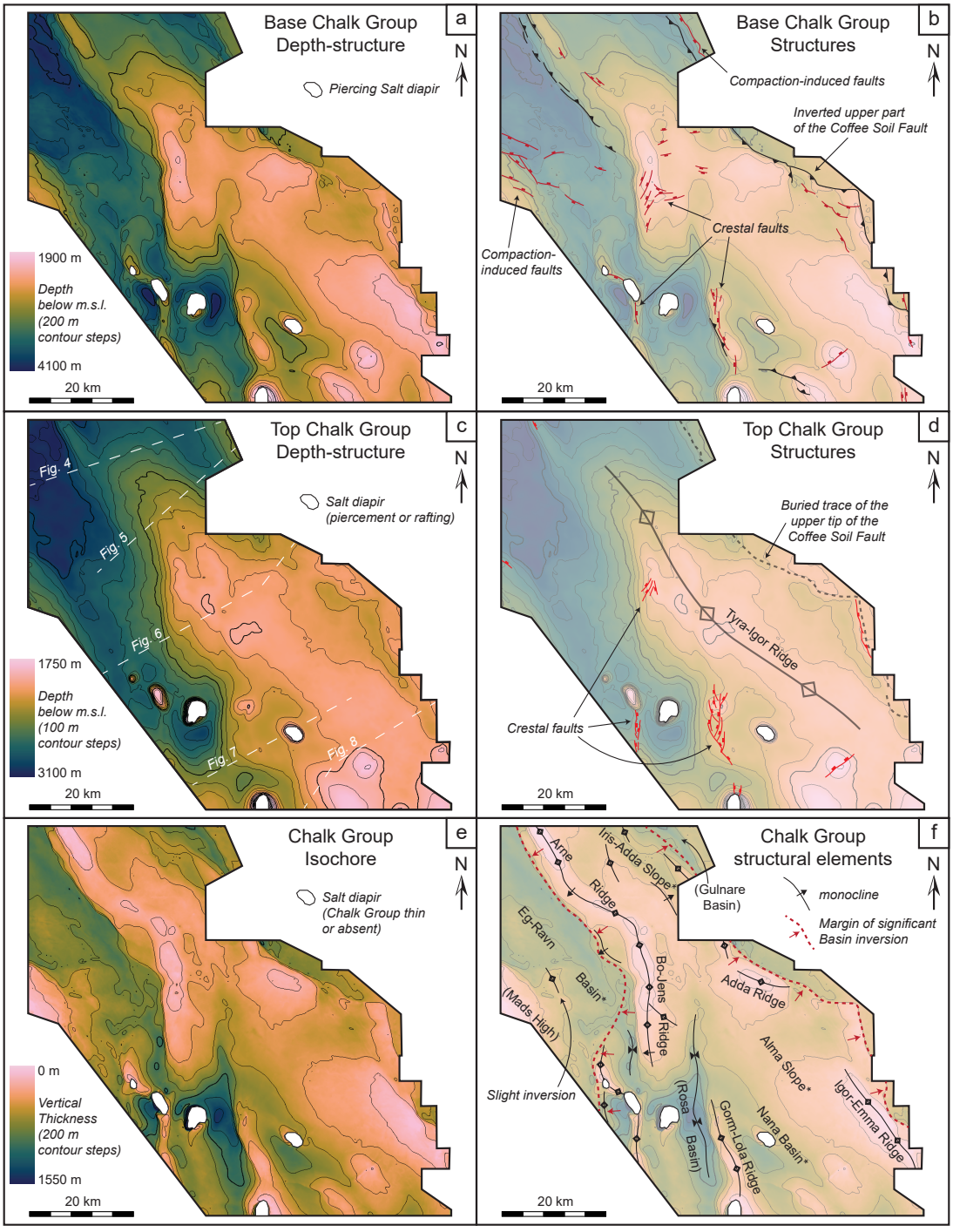

https://doi.org/10.5194/se-2020-127
Preprint. Discussion started: 27 August 2020
© Author(s) 2020. CC BY 4.0 License.

Solid Earth
Discussions
Open Access
EGU

Figure 11: Depth- and structure maps constructed from seismic data illustrating the deformational geometries of the base and top of the Chalk Group (Late Cretaceous, syn-inversion). (a) Base Chalk Group depth and (b) –structures. A high number of smaller normal faults offset this surface. These were induced mostly from compaction or crestal collapse above inversion structrures, i.e. local extension; (c) Top Chalk Group depth and (d) –structures. Note the expression of the Tyra-Igor Ridge which formed due Paleogene basin inversion. Crestal faults are evident above some prominent inversion ridges. (e) Chalk Group isochore (thickness) map and (d) –structural elements. This illustrates the marked change in subsidence patterns compared to the pre-inversion basin (Figs. 10c and 10d). Now, depocentres are located outside the zone affected by significant inversion while thinning occurs above areas of relative uplift. Names in brackets indicate preexisting structural elements; * = names from Jakobsen (2014). An overview of the stratigraphic units and mapped surfaces is found in Fig. 3. The colour scale used (Batlow) was constructed by Crameri (2018).

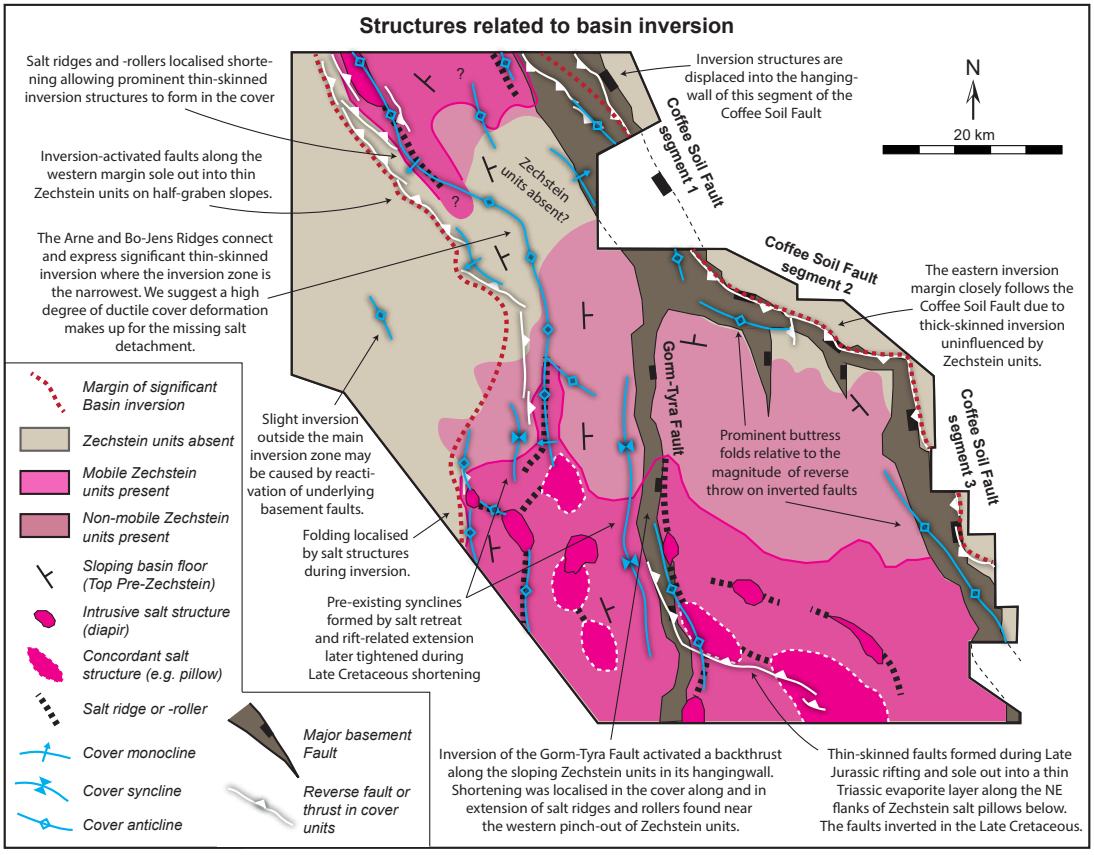

Figure 12: Overview of active structures during Late Cretaceous basin inversion in the study area. This illustrates the spatial relationships between the main sub-salt basement structures, Zechstein units and salt structures, and inversion structures in the cover units. Note the concentration of thin-skinned inversion structures along the western pinch-out of the Zechstein units and directly above the adjacent salt ridges and –rollers. Note the different expressions of inversion or lack thereof directly above the major basement-fault tips. Reverse reactivation of the Coffee Soil Fault segment 1 and the Gorm-Tyra Fault is inferred in order to balance the thin-skinned shortening expressed along the western margin of the inversion zone. See text for explanation.

https://doi.org/10.5194/se-2020-127
Preprint. Discussion started: 27 August 2020
© Author(s) 2020. CC BY 4.0 License.

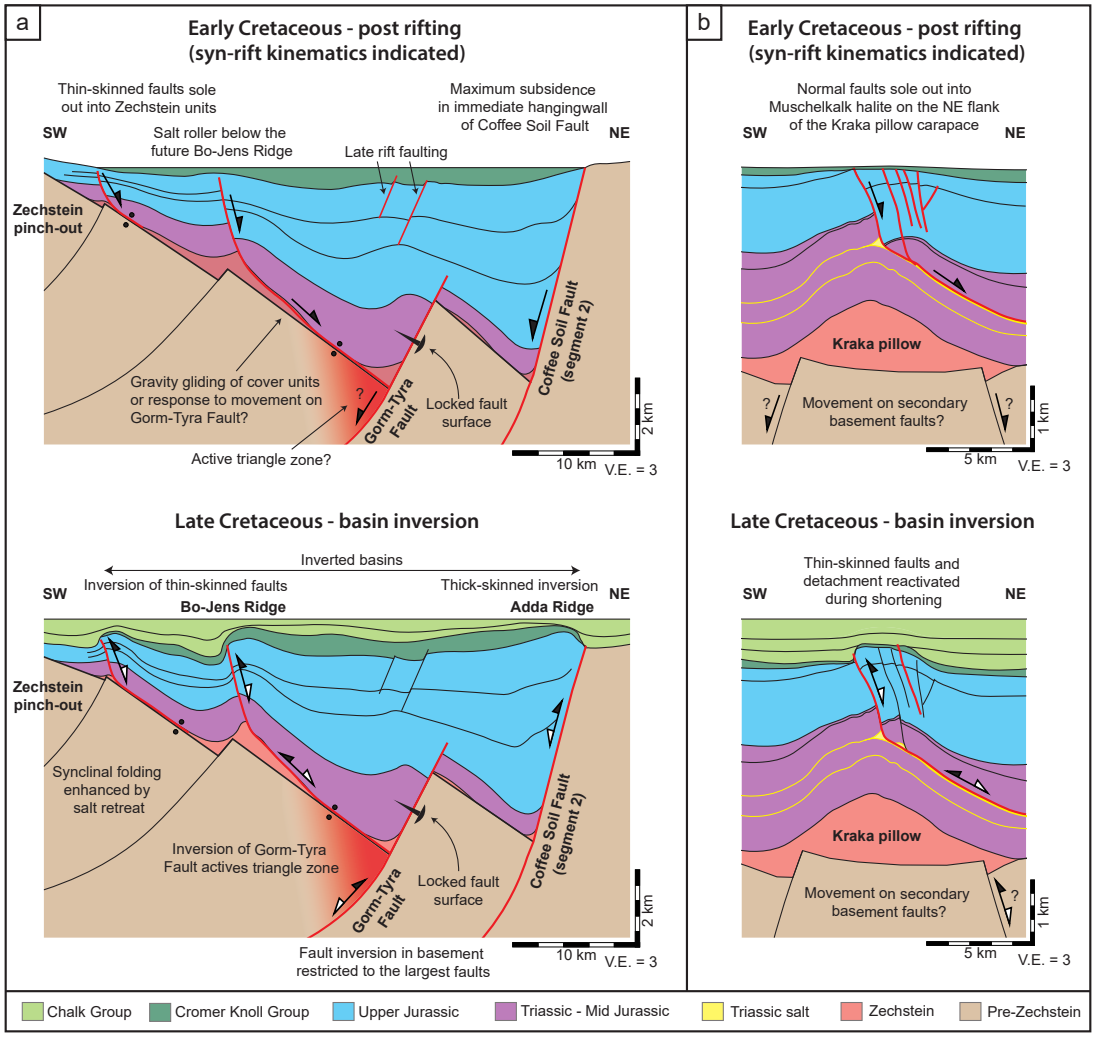

Figure 13: Simplified 2D sections illustrating the development of various structural styles of basin inversion from the pre-inversion rift basins in our study area. Active faults are indicated in red. Note the different scales for the two sections. (a) Section constructed from the interpretation seen in in Fig. 6 (See Fig. 1 for location). The western margin of inversion is characterised by thin-skinned inversion with Zechstein units acting as detachment. Thin-skinned structures initially developed during rifting at the pinch-out of the Zechstein units and above salt ridges. Thick-skinned inversion of the Coffee Soil Fault formed e.g. the Adda Ridge along the eastern margin. Inversion of the deeper Gorm-Tyra fault caused a triangle zone (indicated by red area) to develop with a thrust detachment through the thin Zechstein units along the basin floor. The upper part of the Gorm-Tyra Fault did not reactivate and hence, no inversion structures formed directly above it. Instead, shortening was accommodated in the cover units by inversion of the thin-skinned faults soling out into Zechstein units. This mechanism is inferred also for segment 1 of the Coffee Soil Fault and the development of Arne Ridge (Fig. 4). (b) Section constructed from the interpretation seen in Fig. 8 (See Fig. 1 for location), illustrating the Kraka structure before and after Late Cretaceous inversion. Note the detachment in a Triassic salt unit (Muschelkalk Halite).